Optics Communications 444 (2019) 172–183

Contents lists available at ScienceDirect

Optics Communications

journal homepage: www.elsevier.com/locate/optcom

On the performance of a multi-user multi-hop hybrid FSO/RF communication system

Mohammad Ali Amirabadi, Vahid Tabataba Vakili *

School of Electrical Engineering, Iran University of Science and Technology (IUST), Tehran 1684613114, Iran

ARTICLE INFO

Keywords:
Free Space Optical / Radio Frequency
Multi-Hop
Gamma–Gamma
Negative Exponential
Pointing Error

ABSTRACT

One of the main problems in mobile communication systems is long-range impassable links or some specific atmospheric conditions under which Radio Frequency (RF) connection becomes easily disrupted. One way to solve this problem is by consuming more power or adding processing complexity, but a small user mobile phone cannot deserve more complexity or power supply. Another way is to use an access point that amplifies received signal via short-range RF link and forwards it to via long-range Free Space Optical (FSO) link. In this paper, a novel multi-user multi-hop hybrid FSO / RF communication system is presented. This structure consists of two main parts. The first part establishes the connection between the mobile users and the source base station, and the second part establishes the connection between the source and the destination base stations. In the first part, mobile users want to connect to the source base station via a long-range link; therefore, an amplify and forward relay is used for communication establishment. In the second part, the source and the destination base stations are connected via a multi-hop hybrid parallel FSO / RF link with demodulating and forward relaying. The FSO link in moderate to strong and in saturated regimes is assumed at Gamma–Gamma and Negative Exponential atmospheric turbulence, respectively, also the effect of pointing error is considered, and RF link has Rayleigh fading. New closed-form exact and asymptotic expressions are derived for the Outage Probability and Bit Error Rate (BER) of the proposed structure. Derived expressions are verified with MATLAB simulations. The proposed structure has advantages of FSO, RF, relay-assisted, and multi-user systems at the same time. Results indicate that it has low dependence on the number of users and the number of relays. Therefore, it is suitable for areas with varying population and long-range links. This structure offers independent performance without additional power consumption, processing latency, and complexity. The innovations and contributions of this paper, which are first introduced in the multi-hop hybrid FSO / RF hybrid structure, include the novelty of the proposed structure, the presentation of new exact and asymptotic mathematical solutions, use of multi-user scheme in a multi-hop FSO / RF structure, BER analysis, using amplify and forward as well as decode and forward protocols, taking into account a wide range of atmospheric turbulence with the effect of pointing error, using opportunistic selection schemes at each relay.

1. Introduction

Intensity Modulation/Direct Detection (IM/DD) based on on–off keying is often used in Free Space Optical (FSO) communication system. The fact that the detection threshold of this modulation changes based on atmospheric turbulence intensity makes it suitable for areas with a frequent change in atmospheric turbulence intensity [1].

During the last decades, the FSO system has attracted many considerations due to advances in optoelectronic devices and reduction of their costs. The FSO system has a large bandwidth and is highly secure, simple, cheap, and suitable for the last-mile backup application in 4G and 5G systems [2].

One of the main challenges toward the FSO system is its high sensitivity to atmospheric turbulence. Atmospheric turbulence causes random fluctuations in the received signal intensity [3]. The misalignment of trans-receiver, which is caused by building sway, little earthquakes, etc., is called the effect of pointing error, and can significantly degrade the performance of FSO system. Various statistical distributions can be used in order to investigate the effects of atmospheric turbulences e.g., Exponential-Weibull [4], Generalized Malaga [5], Log-normal [6], Gamma–Gamma [7], and Negative Exponential [8]. Among them, Gamma–Gamma and Negative Exponential are highly accompanied by experimental results for moderate to strong and saturated atmospheric turbulence regimes, respectively.

Weather conditions have different effects on the performance of FSO and Radio Frequency (RF) links [9]. Actually, these two links are complementary to each other [10]. Accordingly, their combination

* Corresponding author.
E-mail address: m_amirabadi@elec.iust.ac.ir (V.T. Vakili).

https://doi.org/10.1016/j.optcom.2019.03.070
Received 16 February 2019; Received in revised form 11 March 2019; Accepted 26 March 2019
Available online 8 April 2019

would have advantages of both of them, e.g. reliability and accessibility, at the same time.

The investigations on the so-called hybrid FSO/RF system can be divided into three main categories. The first category deals with single-hop parallel FSO/RF structure [9,11–17]. These works investigated the single-user scheme, except [9], which used a multi-user structure [9]. The second category investigates the performance of dual-hop structure [5,7,18–25]. These works used either FSO or RF link at each hop, except [20] that used a direct backup link between source and destination. The last category deals with multi-hop structure. This category has been investigated in the FSO system [26–30], but in the FSO/RF system it is still a new topic [31–34]. These works implemented a single-user multi-hop hybrid parallel [32] or series [31,33,34] FSO/RF system and investigated Outage Probability of the system. The main contributions and novelties of this paper include presenting a new structure, different first hop structure, multi-user communication, signal selection at each hop, amplify and forward plus demodulate and forward relaying, considering a wide atmospheric turbulence range from moderate to saturated with the effect of pointing error.

Various relaying protocols have been used for hybrid FSO/RF systems; they include decode and forward [19], amplify and forward [35], quantize and forward [20]. Amplify and forward relaying is done either by fixed or by adaptive gain. The fixed gain amplification has less complexity but more power dissipation. Therefore, when Channel State Information (CSI) is unknown, it is better to use fixed gain amplification, but when CSI is known, the adaptive gain amplification is a better choice [20]. Generally speaking, demodulate and forward has lower power consumption, also amplify and forward enhances noise power. Therefore, in short-range links, demodulate and forward protocol is preferred. it is only recommended in long-range links where establishing the connection is more important than power consumption or complexity of the system.

In this paper, a novel multi-user multi-hop hybrid FSO/RF system is presented, which is consisted of two main parts. The main motivation of presenting this structure is that RF connection disrupts easily in long-range impassable areas or under some specific atmospheric conditions. Although these effects could be mitigated by consuming more power or adding complex processing, a small mobile phone battery cannot deserve much complexity or power consumption. Usually, in this situations relay assisted systems could help to install the connection. In addition, complementariness of FSO and RF links brings a new solution in mind. An access point that amplifies the received signal from the user via short-range RF link and forwards it to the Base Station via long-range FSO link, could solve both of the mentioned problems.

At the first part of the proposed structure, mobile users transmit RF signals to an access point via a short-range RF link. Between received signals, the signal with the maximum Signal to Noise Ratio (SNR) is selected, amplified and forwarded to source Base Station through an FSO link. The second part connects source and destination Base Stations through a multi-hop parallel FSO/RF link. At each hop, the signal is transmitted simultaneously from both FSO and RF transmitters. The multi-hop structure consists of many short links; therefore, demodulate and forward protocol is used in it.

The FSO link, in moderate to strong and in saturated regimes, has Gamma–Gamma and Negative Exponential atmospheric turbulence, respectively. In order to get closer to the actual results, the effect of pointing error is also considered. Fading of the RF link has Rayleigh distribution. New closed-form exact and asymptotic expressions are derived for Bit Error Rate (BER) and Outage Probability of the proposed structure for Differential Binary Phase Shift Keying (DBPSK) modulation. Derived expressions are validated through MATLAB simulations.

The remainder of this paper is organized as follows: system model is expressed in Section 2. Performances of known CSI and unknown CSI schemes are investigated in Sections 3 and 4, respectively. In Section 5 simulation and analytical results are compared. Section 6 is the conclusions of this study.

2. System model

The proposed multi-hop hybrid FSO/RF system is presented in Fig. 1. Considering x_i as the transmitted RF signal from the ith mobile user, the received signal at the access point (first relay) becomes as follows [9]:

$$y_{1,i} = x_i h_{1,i} + e_{1,i}, \tag{1}$$

where $h_{1,i}$ is the fading coefficient of RF channel between the ith user and access point, $e_{1,i}$ is additive white Gaussian noise (AWGN) with zero mean and σ^2_{RF} variance. At each time slot, between received RF signals, the access point selects the signal with maximum SNR. The selected RF signal (y_1) is converted to an FSO signal by conversion efficiency of η, and then added by a unit amplitude bias; this bias addition is to ensure that the FSO signal is not negative. The biased FSO signal is amplified and forwarded in the following form [25]:

$$x_2 = G\left(1 + \eta y_1\right), \tag{2}$$

where G is the amplification gain. After removing the biased component, the received signal at the source Base Station (second relay) becomes as follows [25]:

$$y_2 = G\eta I_2 h_1 x + G\eta I_2 e_1 + e_2, \tag{3}$$

where I_2 is the irradiance intensity of FSO channel, e_2 is AWGN with zero mean and σ^2_{FSO} variance. Assuming that the transmitted signal has unit energy $\left(\text{i.e.} E\left[x^2\right] = 1\right)$, instantaneous SNR at the second relay input becomes as follows [18]:

$$\gamma_{2^{nd}relay} = \frac{G^2\eta^2 I_2^2 h_1^2}{G^2\eta^2 I_2^2 \sigma^2_{RF} + \sigma^2_{FSO}}. \tag{4}$$

When CSI is known at the access point, the amplification gain could change adaptively according to the CSI and could be written as $G^2 = 1/(h_1^2 + \sigma^2_{RF})$ [36]. The output signal power of this scheme is fixed. Substituting $\gamma_1 = h_1^2/\sigma^2_{RF}$, $\gamma_2 = G^2\eta^2 I_2^2/\sigma^2_{FSO}$, and G, the end-to-end SNR at the source Base Station input becomes as follows [18]:

$$\gamma_{2^{nd}relay} = \frac{\gamma_1\gamma_2}{\gamma_1 + \gamma_2 + 1}. \tag{5}$$

Regarding the fixed gain amplification, it could be written as $G^2 = 1/(C\sigma^2_{RF})$, where C is a desired constant parameter [36]. Substituting $\gamma_1 = h_1^2/\sigma^2_{RF}$, $\gamma_2 = G^2\eta^2 I_2^2/\sigma^2_{FSO}$, and G into (4), the end-to-end SNR at the source Base Station input becomes as follows [5]:

$$\gamma_{2^{nd}relay} = \frac{\gamma_1\gamma_2}{C + \gamma_2}. \tag{6}$$

As discussed earlier, amplify and forward relaying, due to its power consumption and noise enhancement, is recommended only in situations that connection establishment is more important than power consumption or processing complexity. At the second part of the proposed structure, source and destination Base Stations are connected with multiple short hops without any connection problem. Therefore, demodulate and forward relaying, due to its simplicity and low power consumption is implemented at each relay station.

The received signal at the source Base Station (y_2) is first demodulated, regenerated, then modulated, duplicated, and finally forwarded through parallel hybrid FSO/RF link. At each hop, FSO channel has irradiance intensity of $I_j; j = 3, 4, \ldots, M + 1$, where M is the number of relays, and RF channel has fading coefficient of h_j. The received FSO and RF signals at each relay input are added by AWGN, with zero mean and σ^2_{FSO} and σ^2_{RF} variances. The signal with higher SNR is demodulated, regenerated, then modulated, duplicated, and finally forwarded through parallel hybrid FSO/RF link. The same procedure will be repeated at each hop until reaching the destination Base Station.

In IM/DD, the probability density function (pdf) and Cumulative Distribution Function (CDF) of Gamma–Gamma distribution with the

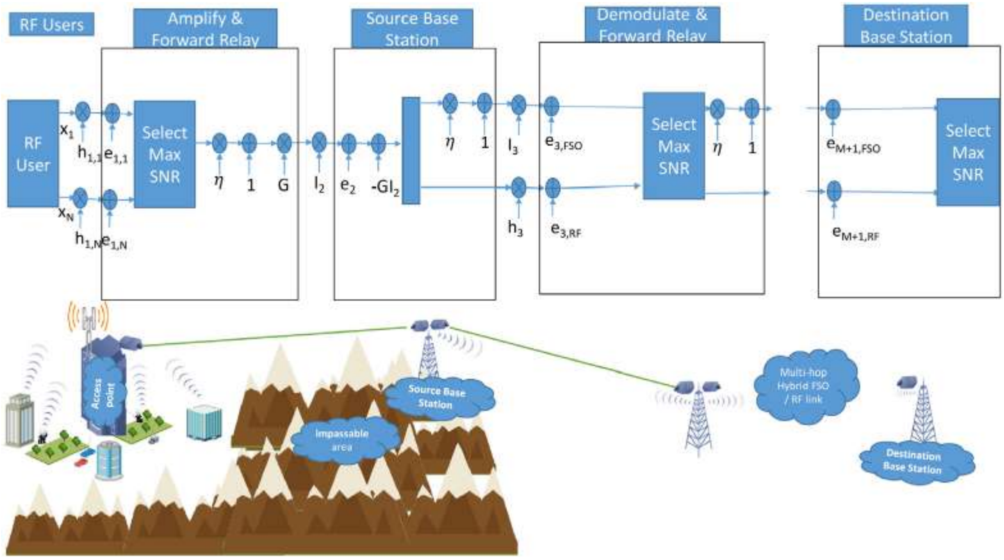

Fig. 1. The proposed multi-hop relay-assisted hybrid FSO/RF system.

effect of pointing error and the CDF of Rayleigh distribution are respectively as follows [21]:

$$f_{\gamma_{FSO}}(\gamma)=\frac{\xi^2}{2\Gamma(\alpha)\Gamma(\beta)\gamma}G_{1,4}^{3,0}\left(\alpha\beta\kappa\sqrt{\frac{\gamma}{\bar{\gamma}_{FSO}}}\middle|\begin{matrix}\xi^2+1\\ \xi^2,\alpha,\beta\end{matrix}\right), \tag{7}$$

$$F_{\gamma_{FSO}}(\gamma)=\frac{\xi^2}{\Gamma(\alpha)\Gamma(\beta)}G_{2,4}^{3,1}\left(\alpha\beta\kappa\sqrt{\frac{\gamma}{\bar{\gamma}_{FSO}}}\middle|\begin{matrix}1,\xi^2+1\\ \xi^2,\alpha,\beta,0\end{matrix}\right), \tag{8}$$

$$F_{\gamma_{RF}}(\gamma)=1-e^{-\frac{\gamma}{\bar{\gamma}_{RF}}}, \tag{9}$$

where $G_{p,q}^{m,n}\left(z\middle|\begin{matrix}a_1,a_2,\dots,a_p\\ b_1,b_2,\dots,b_q\end{matrix}\right)$ is Meijer-G function [37, Eq. 07.34.02.0001.01], $\Gamma(.)$ is Gamma function [37, Eq. 06.05.02.0001.01], $\xi^2=\omega_{Z_{eq}}/(2\sigma_s)$ is the ratio of the equivalent received beam radius $(\omega_{Z_{eq}}/2)$ to the standard deviation of pointing errors at the receiver (σ_s), $\kappa=\frac{\xi^2}{\xi^2+1}$, $\alpha=\left[\exp\left(0.49\sigma_R^2/\left(1+1.11\sigma_R^{12/5}\right)^{7/6}\right)-1\right]^{-1}$ and $\beta=\left[\exp\left(0.51\sigma_R^2/\left(1+0.69\sigma_R^{12/5}\right)^{5/6}\right)-1\right]^{-1}$ are parameters related to Gamma–Gamma atmospheric turbulence, where σ_R^2 is Rytov variance [24]. Average electrical SNR in the FSO link is represented by $\bar{\gamma}_{FSO}=\eta^2E(I^2)/\sigma_{FSO}^2=\eta^2/\sigma_{FSO}^2$ [25].

From Appendix A, the CDF of Negative Exponential atmospheric turbulence with the effect of pointing error is as follows:

$$F_{\gamma_{\mathrm{FSO}}}(\gamma)=W\gamma^{\frac{\xi^2-1}{2}}G_{2,3}^{2,1}\left(\frac{\lambda}{A_0}\sqrt{\frac{\gamma}{\bar{\gamma}_{FSO}}}\middle|\begin{matrix}1-\xi^2,1\\ 0,2-\xi^2,-\xi^2\end{matrix}\right). \tag{10}$$

Users are located separately, hence transmitted RF signals experience independent fading. Therefore, it would be highly probable that at least one RF signal experience a favorable channel condition. Generally speaking, in multi-user structures, granting the channel access to the best user would improve performance, and results in the so-called multi-user diversity gain. Considering the best user as the user with the best link quality (maximum SNR), the CDF of the instantaneous SNR at the access point input (γ_1) becomes as follows [38]:

$$\begin{aligned}F_{\gamma_1}(\gamma)&=\Pr\left(\max\left(\gamma_{1,1},\gamma_{1,2},\dots,\gamma_{1,N}\right)\le\gamma\right)\\&=\Pr\left(\gamma_{1,1}\le\gamma,\gamma_{1,2}\le\gamma,\dots,\gamma_{1,N}\le\gamma\right),\end{aligned} \tag{11}$$

where $\gamma_{1,\mathrm{i}}$ is instantaneous SNR at the access point input of ith path. Assuming independent identical distribution for RF paths, and using (9), the CDF of instantaneous SNR at the access point input becomes as follows [21]:

$$F_{\gamma_1}(\gamma)=\prod_{\mathrm{i}=1}^{\mathrm{N}}F_{\gamma_{1,i}}(\gamma)=\left(F_{\gamma_{1,i}}(\gamma)\right)^N=\left(1-e^{-\frac{\gamma}{\bar{\gamma}_{RF}}}\right)^N. \tag{12}$$

Differentiating (12), the pdf of instantaneous SNR at the access point input becomes as follows [21]:

$$f_{\gamma_1}(\gamma)=\frac{N}{\bar{\gamma}_{RF}}e^{-\frac{\gamma}{\bar{\gamma}_{RF}}}\left(1-e^{-\frac{\gamma}{\bar{\gamma}_{RF}}}\right)^{N-1}=\sum_{k=0}^{N-1}\binom{N-1}{k}(-1)^k\frac{N}{\bar{\gamma}_{RF}}e^{-\frac{(k+1)\gamma}{\bar{\gamma}_{RF}}}. \tag{13}$$

In order to have better performance, between received FSO and RF signals at each relay, one with higher SNR is selected. Accordingly, the CDF of the instantaneous SNR at jth relay input (γ_j) becomes as follows [38]:

$$\begin{aligned}F_{\gamma_j}(\gamma)&=\Pr\left(\max\left(\gamma_{\gamma_{FSO},j},\gamma_{\gamma_{RF},j}\right)\le\gamma\right)=\Pr\left(\gamma_{\gamma_{FSO},j}\le\gamma,\gamma_{\gamma_{RF},j}\le\gamma\right)\\&=F_{\gamma_{FSO},j}(\gamma)F_{\gamma_{RF},j}(\gamma),\end{aligned} \tag{14}$$

where the last equality appears because FSO and RF links are assumed independent.

3. Performance of known CSI scheme

Assuming high SNR approximation, (5) becomes equal to [18]:

$$\gamma_{2^{nd}relay}=\frac{\gamma_1\gamma_2}{\gamma_1+\gamma_2+1}\cong\min\left(\gamma_1,\gamma_2\right). \tag{15}$$

Therefore, the CDF of $\gamma_{2^{nd}relay}$ random variable becomes as [25]:

$$\begin{aligned}F_{\gamma_{2^{nd}relay}}(\gamma)&=\Pr\left(\gamma_{2^{nd}relay}\le\gamma\right)\\&=1-\Pr\left(\min\left(\gamma_1,\gamma_2\right)\ge\gamma\right)=1-\Pr\left(\gamma_1\ge\gamma\right)\Pr\left(\gamma_2\ge\gamma\right)=1-\left(1-F_{\gamma_1}(\gamma)\right)\left(1-F_{\gamma_2}(\gamma)\right).\end{aligned} \tag{16}$$

Substituting (8) and (12) into (16), and by using binomial expansion theorem, the CDF of $\gamma_{2^{nd}relay}$ in Gamma–Gamma atmospheric turbulence with the effect of pointing error becomes as follows [21]:

$$\begin{aligned}F_{\gamma_{2^{nd}relay}}(\gamma)&=1+\sum_{k=1}^{N}\binom{N}{k}(-1)^k e^{-\frac{k\gamma}{\bar{\gamma}_{RF}}}\\&\times\left(1-\frac{\xi^2}{\Gamma(\alpha)\Gamma(\beta)}G_{2,4}^{3,1}\left(\alpha\beta\kappa\sqrt{\frac{\gamma}{\bar{\gamma}_{FSO}}}\middle|\begin{matrix}1,\xi^2+1\\ \xi^2,\alpha,\beta,0\end{matrix}\right)\right)\end{aligned} \tag{17}$$

Substituting (10) and (12) into (16), and using binomial expansion theorem, the CDF of $\gamma_{2^{nd}relay}$ in Negative Exponential atmospheric turbulence with the effect of pointing error becomes as follows:

$$F_{\gamma_{2^{nd}relay}}(\gamma) = 1 + \sum_{k=1}^{N} \binom{N}{k} (-1)^k e^{-\frac{k\gamma}{\bar{\gamma}_{RF}}} \times \left(1 - W\gamma^{\frac{\xi^2-1}{2}} G_{2,3}^{2,1}\left(\frac{\lambda}{A_0}\sqrt{\frac{\gamma}{\bar{\gamma}_{FSO}}}\middle| \begin{matrix} 1-\xi^2, 1 \\ 0, 2-\xi^2, -\xi^2 \end{matrix}\right)\right). \tag{18}$$

3.1. Outage probability

In the proposed structure, an outage occurs when the instantaneous SNR at each relay input falls down below a threshold level. Accordingly, the Outage Probability of the proposed structure becomes as follows [38]:

$$\begin{aligned} P_{out}(\gamma_{th}) &= \Pr\left\{(\gamma_1, \gamma_2, \ldots, \gamma_{M+1}) \le \gamma_{th}\right\} \\ &= 1 - \Pr\left\{\gamma_1 \ge \gamma_{th}, \gamma_2 \ge \gamma_{th}, \ldots, \gamma_{M+1} \ge \gamma_{th}\right\} \\ &= 1 - (1 - \Pr\left\{(\gamma_1, \gamma_2) \le \gamma_{th}\right\})(1 - \Pr\left\{(\gamma_3 \le \gamma_{th})\right\}) \\ &\quad \cdots (1 - \Pr\left\{(\gamma_{M+1} \le \gamma_{th})\right\}) \\ &= 1 - \left(1 - F_{\gamma_{2^{nd}relay}}(\gamma_{th})\right)\left(1 - F_{\gamma_3}(\gamma_{th})\right) \cdots \left(1 - F_{\gamma_{M+1}}(\gamma_{th})\right), \end{aligned} \tag{19}$$

where the last equality appears because $P_{out}(\gamma_{th}) = F_\gamma(\gamma_{th})$. Considering (14), and after substituting (17), (8) and (9) into (19), Outage Probability of the proposed structure in Gamma–Gamma atmospheric turbulence with the effect of pointing error becomes equal to:

$$\begin{aligned} P_{out}(\gamma_{th}) &= 1 + \sum_{k=1}^{N} \binom{N}{k} (-1)^k e^{-\frac{k\gamma_{th}}{\bar{\gamma}_{RF}}} \\ &\times \left(1 - \frac{\xi^2}{\Gamma(\alpha)\Gamma(\beta)} G_{2,4}^{3,1}\left(\alpha\beta\kappa\sqrt{\frac{\gamma_{th}}{\bar{\gamma}_{FSO}}}\middle| \begin{matrix} 1, \xi^2+1 \\ \xi^2, \alpha, \beta, 0 \end{matrix}\right)\right) \\ &\times \left[1 - \frac{\xi^2}{\Gamma(\alpha)\Gamma(\beta)}\left(1 - e^{-\frac{\gamma_{th}}{\bar{\gamma}_{RF}}}\right)\right. \\ &\left.\times G_{2,4}^{3,1}\left(\alpha\beta\kappa\sqrt{\frac{\gamma_{th}}{\bar{\gamma}_{FSO}}}\middle| \begin{matrix} 1, \xi^2+1 \\ \xi^2, \alpha, \beta, 0 \end{matrix}\right)\right]^{M-1}. \end{aligned} \tag{20}$$

In part B (next part) the Outage Probability is used for BER calculation; but (20) a bit rigid. Therefore, it is better to do some mathematical simplifications on it. Substituting binomial expansion of $\left[1 - \frac{\xi^2}{\Gamma(\alpha)\Gamma(\beta)}\left(1 - e^{-\frac{\gamma_{th}}{\bar{\gamma}_{RF}}}\right) G_{2,4}^{3,1}\left(\alpha\beta\kappa\sqrt{\frac{\gamma_{th}}{\bar{\gamma}_{FSO}}}\middle| \begin{matrix} 1, \xi^2+1 \\ \xi^2, \alpha, \beta, 0 \end{matrix}\right)\right]^{M-1}$ as $\sum_{t=0}^{M-1}\sum_{u=0}^{t}\binom{M-1}{t}\binom{t}{u} \times (-1)^{t+u} e^{-\frac{u\gamma_{th}}{\bar{\gamma}_{RF}}}\left(\frac{\xi^2}{\Gamma(\alpha)\Gamma(\beta)} G_{2,4}^{3,1}\left(\alpha\beta\kappa\sqrt{\frac{\gamma_{th}}{\bar{\gamma}_{FSO}}}\middle| \begin{matrix} 1, \xi^2+1 \\ \xi^2, \alpha, \beta, 0 \end{matrix}\right)\right)^t$, Outage Probability of the proposed structure in Gamma–Gamma atmospheric turbulence with the effect of pointing error becomes equal to:

$$\begin{aligned} P_{out}(\gamma_{th}) &= 1 + \sum_{k=1}^{N}\sum_{t=0}^{M-1}\sum_{u=0}^{t} \Omega_1 e^{-\frac{(k+u)\gamma_{th}}{\bar{\gamma}_{RF}}} \\ &\times \left(\frac{\xi^2}{\Gamma(\alpha)\Gamma(\beta)} G_{2,4}^{3,1}\left(\alpha\beta\kappa\sqrt{\frac{\gamma_{th}}{\bar{\gamma}_{FSO}}}\middle| \begin{matrix} 1, \xi^2+1 \\ \xi^2, \alpha, \beta, 0 \end{matrix}\right)\right)^t \\ &\times \left[1 - \frac{\xi^2}{\Gamma(\alpha)\Gamma(\beta)} G_{2,4}^{3,1}\left(\alpha\beta\kappa\sqrt{\frac{\gamma_{th}}{\bar{\gamma}_{FSO}}}\middle| \begin{matrix} 1, \xi^2+1 \\ \xi^2, \alpha, \beta, 0 \end{matrix}\right)\right]. \end{aligned} \tag{21}$$

where $\Omega_1 = \binom{N}{k}\binom{M-1}{t}\binom{t}{u}(-1)^{k+t+u}$.

Considering (14), and after substituting (18), (9) and (10) into (19), Outage Probability of the proposed structure in Negative Exponential atmospheric turbulence with the effect of pointing error becomes equal to:

$$\begin{aligned} P_{out}(\gamma_{th}) &= 1 + \sum_{k=1}^{N} \binom{N}{k} (-1)^k e^{-\frac{k\gamma_{th}}{\bar{\gamma}_{RF}}} \\ &\times \left(W\gamma_{th}^{\frac{\xi^2-1}{2}} G_{2,3}^{2,1}\left(\frac{\lambda}{A_0}\sqrt{\frac{\gamma_{th}}{\bar{\gamma}_{FSO}}}\middle| \begin{matrix} 1-\xi^2, 1 \\ 0, 2-\xi^2, -\xi^2 \end{matrix}\right)\right) \\ &\times \left[1 - \left(1 - e^{-\frac{\gamma_{th}}{\bar{\gamma}_{RF}}}\right) W\gamma_{th}^{\frac{\xi^2-1}{2}} G_{2,3}^{2,1}\left(\frac{\lambda}{A_0}\sqrt{\frac{\gamma_{th}}{\bar{\gamma}_{FSO}}}\middle| \begin{matrix} 1-\xi^2, 1 \\ 0, 2-\xi^2, -\xi^2 \end{matrix}\right)\right]^{M-1}. \end{aligned} \tag{22}$$

Substituting binomial expansion of $\left[1 - \left(1 - e^{-\frac{\gamma_{th}}{\bar{\gamma}_{RF}}}\right) W\gamma_{th}^{\frac{\xi^2-1}{2}} G_{2,3}^{2,1}\left(\frac{\lambda}{A_0}\sqrt{\frac{\gamma_{th}}{\bar{\gamma}_{FSO}}}\middle| \begin{matrix} 1-\xi^2, 1 \\ 0, 2-\xi^2, -\xi^2 \end{matrix}\right)\right]^{M-1}$ as $\sum_{t=0}^{M-1}\sum_{u=0}^{t}\binom{M-1}{t}\binom{t}{u}(-1)^{t+u} e^{-\frac{u\gamma_{th}}{\bar{\gamma}_{RF}}}\left(W\gamma_{th}^{\frac{\xi^2-1}{2}} G_{2,3}^{2,1}\left(\frac{\lambda}{A_0}\sqrt{\frac{\gamma_{th}}{\bar{\gamma}_{FSO}}}\middle| \begin{matrix} 1-\xi^2, 1 \\ 0, 2-\xi^2, -\xi^2 \end{matrix}\right)\right)^t$, Outage Probability of the proposed structure in Negative Exponential atmospheric turbulence with the effect of pointing error becomes equal to:

$$\begin{aligned} P_{out}(\gamma_{th}) &= 1 + \\ &\sum_{k=1}^{N}\sum_{t=0}^{M-1}\sum_{u=0}^{t} \Omega_2 e^{-\frac{(k+u)\gamma_{th}}{\bar{\gamma}_{RF}}}\left(W\gamma_{th}^{\frac{\xi^2-1}{2}} G_{2,3}^{2,1}\right. \\ &\left.\times\left(\frac{\lambda}{A_0}\sqrt{\frac{\gamma_{th}}{\bar{\gamma}_{FSO}}}\middle| \begin{matrix} 1-\xi^2, 1 \\ 0, 2-\xi^2, -\xi^2 \end{matrix}\right)\right)^t \left[1 - \right. \\ &\left. W\gamma_{th}^{\frac{\xi^2-1}{2}} G_{2,3}^{2,1}\left(\frac{\lambda}{A_0}\sqrt{\frac{\gamma_{th}}{\bar{\gamma}_{FSO}}}\middle| \begin{matrix} 1-\xi^2, 1 \\ 0, 2-\xi^2, -\xi^2 \end{matrix}\right)\right], \end{aligned} \tag{23}$$

where $\Omega_2 = \binom{N}{k}\binom{M-1}{t}\binom{t}{u}(-1)^{k+t+u}$.

3.2. BER

Differential modulations such as DBPSK, are less sensitive to noise and interference, and their detection is optimum because of the following reasons: no need for CSI, no need for feedback to adjust threshold, no effect on system throughput due to lack of pilot or training sequence, reduction in the effects of background noise at the receiver, reduction in the effects of pointing error [23]. The BER of DBPSK modulation could be calculated by the following expression [18]:

$$P_e = \frac{1}{2}\int_0^\infty e^{-\gamma} F_\gamma(\gamma)\, d\gamma = \frac{1}{2}\int_0^\infty e^{-\gamma} P_{out}(\gamma)\, d\gamma \tag{24}$$

Substituting (21) into (24), the BER of DBPSK modulation in Gamma–Gamma atmospheric turbulence with the effect of pointing error becomes as follows:

$$\begin{aligned} P_e &= \frac{1}{2}\int_0^\infty e^{-\gamma}\left\{1 + \sum_{k=1}^{N}\sum_{t=0}^{M-1}\sum_{u=0}^{t} \Omega_1 e^{-\frac{(k+u)\gamma}{\bar{\gamma}_{RF}}}\left(\frac{\xi^2}{\Gamma(\alpha)\Gamma(\beta)} G_{2,4}^{3,1}\right.\right. \\ &\times\left.\left(\alpha\beta\kappa\sqrt{\frac{\gamma}{\bar{\gamma}_{FSO}}}\middle| \begin{matrix} 1, \xi^2+1 \\ \xi^2, \alpha, \beta, 0 \end{matrix}\right)\right)^t \\ &\times\left.\left[1 - \frac{\xi^2}{\Gamma(\alpha)\Gamma(\beta)} G_{2,4}^{3,1}\left(\alpha\beta\kappa\sqrt{\frac{\gamma}{\bar{\gamma}_{FSO}}}\middle| \begin{matrix} 1, \xi^2+1 \\ \xi^2, \alpha, \beta, 0 \end{matrix}\right)\right]\right\} d\gamma. \end{aligned} \tag{25}$$

To the best of the authors' knowledge, there is no solution released for integrating the multiplication of three Meijer-G and one exponential functions. Due to this reason, if $t > 1$, the above integration cannot be solved. In this paper for the first time, exact and asymptotic solutions are developed for this problem. The solution ideas are taken from [39] for the exact solution, and from [25] for the asymptotic solution.

Substituting (53) from Appendix B into (21) derives a new exact form for Outage Probability of the proposed structure; substituting the result into (24) and using [37, Eq. 07.34.21.0088.01], exact BER of

DBPSK modulation in Gamma–Gamma atmospheric turbulence with the effect of pointing error becomes as follows:

$$P_e = \frac{1}{2}\left\{1+\sum_{k=1}^{N}\sum_{t=0}^{M-1}\sum_{u=0}^{t}\sum_{k_1=0}^{t}\sum_{k_2=0}^{k_1}\sum_{n=0}^{\infty}\Omega_1\binom{t}{k_1}\binom{k_1}{k_2}X_0^{t-k_1}\left(Y_n^{(k_1-k_2)} * Z_n^{(k_2)}\right)\frac{\left(\frac{1}{\bar{\gamma}_{FSO}}\right)^{\aleph}}{\left(1+\frac{(k+u)}{\bar{\gamma}_{RF}}\right)^{1+\aleph}}\left[\Gamma(1+\aleph)-\frac{\xi^2 2^{\alpha+\beta-3}}{\pi\Gamma(\alpha)\Gamma(\beta)}G_{5,8}^{6,3}\left(\frac{(\alpha\beta\kappa)^2}{16\bar{\gamma}_{FSO}\left(1+\frac{(k+u)}{\bar{\gamma}_{RF}}\right)}\middle|\begin{matrix}-\aleph,\beth_1\\ \beth_2\end{matrix}\right)\right]\right\}. \tag{26}$$

where $\beth_1=\left(0.5,1,\frac{\xi^2+1}{2},\frac{\xi^2+2}{2}\right)$, $\beth_2=\left(\frac{\xi^2}{2},\frac{\xi^2+1}{2},\frac{\alpha}{2},\frac{\alpha+1}{2},\frac{\beta}{2},\frac{\beta+1}{2},0,\frac{1}{2}\right)$.

Substituting (56) from Appendix C into (21) derives a new asymptotic form for Outage Probability of the proposed structure; substituting the result in (24) and using [37, Eq. 07.34.21.0088.01], asymptotic BER of DBPSK modulation, in Gamma–Gamma atmospheric turbulence with the effect of pointing error becomes as follows:

$$P_e \cong \frac{1}{2}\left\{1+\sum_{k=1}^{N}\sum_{t=0}^{M-1}\sum_{u=0}^{t}\frac{\Omega(\Xi)^t}{\left(1+\frac{k+u}{\bar{\gamma}_{RF}}\right)^{\frac{Ot}{2}+1}}\left[\Gamma\left(\frac{Ot}{2}+1\right)-\frac{\xi^2 2^{\alpha+\beta-3}}{\pi\Gamma(\alpha)\Gamma(\beta)}G_{5,8}^{6,3}\left(\frac{(\alpha\beta\kappa)^2}{16\bar{\gamma}_{FSO}\left(1+\frac{k+u}{\bar{\gamma}_{RF}}\right)}\middle|\begin{matrix}-\frac{Ot}{2},\beth_1\\ \beth_2\end{matrix}\right)\right]\right\}. \tag{27}$$

Substituting (23) into (24), BER of DBPSK modulation in Negative Exponential atmospheric turbulence with the effect of pointing error becomes as follows:

$$P_e = \frac{1}{2}\int_0^{\infty}e^{-\gamma}\left\{1+\sum_{k=1}^{N}\sum_{t=0}^{M-1}\sum_{u=0}^{t}\Omega_2 e^{-\frac{(k+u)\gamma}{\bar{\gamma}_{RF}}}\times\left(W\gamma^{\frac{\xi^2-1}{2}}G_{2,3}^{2,1}\left(\frac{\lambda}{A_0}\sqrt{\frac{\gamma}{\bar{\gamma}_{FSO}}}\middle|\begin{matrix}1-\xi^2,1\\0,2-\xi^2,-\xi^2\end{matrix}\right)\right)^t\times\left[1-W\gamma^{\frac{\xi^2-1}{2}}G_{2,3}^{2,1}\left(\frac{\lambda}{A_0}\sqrt{\frac{\gamma}{\bar{\gamma}_{FSO}}}\middle|\begin{matrix}1-\xi^2,1\\0,2-\xi^2,-\xi^2\end{matrix}\right)\right]\right\}d\gamma. \tag{28}$$

When $t>1$, the above integration is unsolvable; because there is no solution for the integration of multiplication of three Meijer-G and one exponential functions. Substituting (60) from Appendix D into (23), leads to a new exact form of Outage Probability for the proposed structure, substituting the result into (24) and using [37, Eq.07.34.21.0088.01], exact BER of DBPSK modulation in Negative Exponential atmospheric turbulence with the effect of pointing error becomes as follows:

$$P_e = \frac{1}{2}\left\{1+\sum_{k=1}^{N}\sum_{t=0}^{M-1}\sum_{u=0}^{t}\sum_{k_1=0}^{t}\sum_{k_2=0}^{k_1}\sum_{n=0}^{\infty}\Omega_2\binom{t}{k_1}F_0^{t-k_1}E_n^{(k_1)}\left[\frac{\Gamma(1+H)}{\left(1+\frac{k+u}{\bar{\gamma}_{RF}}\right)^{1+H}}-\frac{W2^{-\xi^2}}{\sqrt{\pi}\left(1+\frac{k+u}{\bar{\gamma}_{RF}}\right)^{H}}G_{5,6}^{4,3}\left(\frac{\lambda^2}{4A_0^2\bar{\gamma}_{FSO}\left(1+\frac{k+u}{\bar{\gamma}_{RF}}\right)}\middle|\begin{matrix}1-H,\varrho_1\\ \varrho_2\end{matrix}\right)\right]\right\}. \tag{29}$$

where $\varrho_1=\left(\frac{1-\xi^2}{2},\frac{2-\xi^2}{2},\frac{1}{2},1\right)$, $\varrho_2=\left(0,\frac{1}{2},\frac{2-\xi^2}{2},\frac{3-\xi^2}{2},-\frac{\xi^2}{2},\frac{1-\xi^2}{2}\right)$.

4. Performance of unknown CSI scheme

Using (6), the CDF of end-to-end SNR at the second relay ($\gamma_{2^{nd}relay}$) becomes as follows [21]:

$$F_{\gamma_{2^{nd}relay}}(\gamma)=\Pr\left(\gamma_{FSO}\le\gamma\right)=1-\Pr\left(\gamma_{FSO}\ge\gamma\right)=1-\Pr\left(\frac{\gamma_1\gamma_2}{\gamma_2+C}\ge\gamma\right). \tag{30}$$

After some mathematical simplifications, (30) becomes as follows [24]:

$$F_{\gamma_{2^{nd}relay}}(\gamma)=1-\int_0^{\infty}\Pr\left(\gamma_2\ge\frac{\gamma C}{x}\middle|\gamma_1\right)f_{\gamma_1}(x+\gamma)dx. \tag{31}$$

Substituting (8) and (13) into (31), the CDF of $\gamma_{2^{nd}relay}$ in Gamma–Gamma atmospheric turbulence with the effect of pointing error becomes equal to [21]:

$$F_{\gamma_{2^{nd}relay}}(\gamma)=1-\sum_{k=0}^{N-1}\binom{N-1}{k}(-1)^k\times\frac{N}{\bar{\gamma}_{RF}}e^{-\frac{(k+1)\gamma}{\bar{\gamma}_{RF}}}\int_0^{\infty}e^{-\frac{(k+1)x}{\bar{\gamma}_{RF}}}\left(1-\frac{\xi^2}{\Gamma(\alpha)\Gamma(\beta)}\times G_{2,4}^{3,1}\left(\alpha\beta\kappa\sqrt{\frac{\gamma C}{x\bar{\gamma}_{FSO}}}\middle|\begin{matrix}1,\xi^2+1\\ \xi^2,\alpha,\beta,0\end{matrix}\right)\right)dx. \tag{32}$$

Substituting equivalent Meijer-G form of $G_{2,4}^{3,1}\left(\alpha\beta\kappa\sqrt{\frac{\gamma C}{x\bar{\gamma}_{FSO}}}\middle|\begin{matrix}1,\xi^2+1\\ \xi^2,\alpha,\beta,0\end{matrix}\right)$ as $G_{4,2}^{1,3}\left(\frac{1}{\alpha\beta\kappa}\sqrt{\frac{x\bar{\gamma}_{FSO}}{\gamma C}}\middle|\begin{matrix}1-\xi^2,1-\alpha,1-\beta,1\\0,-\xi^2\end{matrix}\right)$ [37, Eq. 07.34.17.0012.01], and using [37, Eq. 07.34.21.0088.01] and [37, Eq. 07.34.17.0012.01], the CDF of $\gamma_{2^{nd}relay}$ in Gamma–Gamma atmospheric turbulence with the effect of pointing error becomes equal to:

$$F_{\gamma_{2^{nd}relay}}(\gamma)=1-\sum_{k=0}^{N-1}\binom{N-1}{k}(-1)^k\frac{N}{k+1}e^{-\frac{(k+1)\gamma}{\bar{\gamma}_{RF}}}\left[1-\frac{\xi^2 2^{\alpha+\beta-3}}{\pi\Gamma(\alpha)\Gamma(\beta)}G_{4,9}^{7,2}\times\left(\frac{(\alpha\beta\kappa)^2C(k+1)\gamma}{16\bar{\gamma}_{FSO}\bar{\gamma}_{RF}}\middle|\begin{matrix}\psi_1\\ \psi_2\end{matrix}\right)\right] \tag{33}$$

where $\psi_1=\left\{1,\frac{1}{2},\frac{\xi^2+2}{2},\frac{\xi^2+1}{2}\right\}$ and $\psi_2=\left\{\frac{\xi^2}{2},\frac{\xi^2+1}{2},\frac{\alpha}{2},\frac{\alpha+1}{2},\frac{\beta}{2},\frac{\beta+1}{2},0,\frac{1}{2}\right\}$.

Substituting (10) and (13) into (31), the CDF of $\gamma_{2^{nd}relay}$ in Negative Exponential atmospheric turbulence with the effect of pointing error becomes equal to [21]:

$$F_{\gamma_{2^{nd}relay}}(\gamma)=1-\sum_{k=0}^{N-1}\binom{N-1}{k}(-1)^k\frac{N}{\bar{\gamma}_{RF}}e^{-\frac{(k+1)\gamma}{\bar{\gamma}_{RF}}}\int_0^{\infty}e^{-\frac{(k+1)x}{\bar{\gamma}_{RF}}}\times\left(1-W\left(\frac{\gamma c}{x}\right)^{\frac{\xi^2-1}{2}}G_{2,3}^{2,1}\left(\frac{\lambda}{A_0}\sqrt{\frac{\gamma c}{x\bar{\gamma}_{FSO}}}\middle|\begin{matrix}1-\xi^2,1\\0,2-\xi^2,-\xi^2\end{matrix}\right)\right)dx. \tag{34}$$

Substituting equivalent Meijer-G form of $G_{2,3}^{2,1}\left(\frac{\lambda}{A_0}\sqrt{\frac{\gamma c}{x\bar{\gamma}_{FSO}}}\middle|\begin{matrix}1-\xi^2,1\\0,2-\xi^2,-\xi^2\end{matrix}\right)$ as $G_{3,2}^{1,2}\left(\frac{A_0}{\lambda}\sqrt{\frac{x\bar{\gamma}_{FSO}}{\gamma c}}\middle|\begin{matrix}1,\xi^2-1,\xi^2+1\\0,\xi^2\end{matrix}\right)$ [37, Eq. 07.34.17.0012.01], and using [37, Eq. 07.34.21.0088.01] and [33, Eq. 07.34.17.0012.01], the CDF of $\gamma_{2^{nd}relay}$ in Negative Exponential atmospheric turbulence with the effect of pointing error becomes equal to:

$$F_{\gamma_{2^{nd}relay}}(\gamma)=1-\sum_{k=0}^{N-1}\binom{N-1}{k}(-1)^k\frac{N}{k+1}e^{-\frac{(k+1)\gamma}{\bar{\gamma}_{RF}}}\left(1-W(\gamma c)^{\frac{\xi^2-1}{2}}\frac{2^{1-\xi^2}}{\sqrt{\pi}}\left(\frac{k+1}{\bar{\gamma}_{RF}}\right)^{\frac{1-\xi^2}{2}}G_{4,7}^{5,2}\left(\frac{\lambda^2c(k+1)\gamma}{4A_0^2\bar{\gamma}_{FSO}\bar{\gamma}_{RF}}\middle|\begin{matrix}\varphi_1\\ \varphi_2\end{matrix}\right)\right). \tag{35}$$

where $\varphi_1=\left\{\frac{2-\xi^2}{2},\frac{1-\xi^2}{2},1,\frac{1}{2}\right\}$ and $\varphi_2=\left\{\frac{3-\xi^2}{2},\frac{1}{2},0,\frac{3-\xi^2}{2},\frac{2-\xi^2}{2},\frac{1-\xi^2}{2},\frac{-\xi^2}{2}\right\}$.

4.1. Outage probability

According to (14), after substituting (33), (8), and (9) into (19) and by substituting binomial expansion of $\left[1-\frac{\xi^2}{\Gamma(\alpha)\Gamma(\beta)}\left(1-e^{-\frac{\gamma_{th}}{\bar\gamma_{RF}}}\right)G_{2,4}^{3,1}\left(\alpha\beta\kappa\sqrt{\frac{\gamma_{th}}{\bar\gamma_{FSO}}}\middle|\begin{matrix}1,\xi^2+1\\ \xi^2,\alpha,\beta,0\end{matrix}\right)\right]^{M-1}$, Outage Probability of the proposed structure in Gamma–Gamma atmospheric turbulence with the effect of pointing error becomes equal to:

$$P_{out}\left(\gamma_{th}\right)=1-\sum_{k=0}^{N-1}\sum_{t=0}^{M-1}\sum_{u=0}^{t}\Omega_3 e^{-\frac{(k+u+1)\gamma_{th}}{\bar\gamma_{RF}}}\left(\frac{\xi^2}{\Gamma(\alpha)\Gamma(\beta)}\times G_{2,4}^{3,1}\left(\alpha\beta\kappa\sqrt{\frac{\gamma_{th}}{\bar\gamma_{FSO}}}\middle|\begin{matrix}1,\xi^2+1\\ \xi^2,\alpha,\beta,0\end{matrix}\right)\right)^t \times\left[1-\frac{\xi^2 2^{\alpha+\beta-3}}{\pi\Gamma(\alpha)\Gamma(\beta)}G_{4,9}^{7,2}\left(\frac{(\alpha\beta\kappa)^2C(k+1)\gamma_{th}}{16\bar\gamma_{FSO}\bar\gamma_{RF}}\middle|\begin{matrix}\psi_1\\ \psi_2\end{matrix}\right)\right], \tag{36}$$

where $\Omega_3=\binom{N-1}{k}\binom{M-1}{t}\binom{t}{u}(-1)^{k+t+u}\frac{N}{k+1}$.

Substituting (35), (9) and (10) into (19), Outage Probability of the proposed structure in Negative Exponential atmospheric turbulence with the effect of pointing error becomes equal to:

$$P_{out}\left(\gamma_{th}\right)=1-\sum_{k=0}^{N-1}\binom{N-1}{k}(-1)^k\frac{N}{k+1}e^{-\frac{(k+1)\gamma_{th}}{\bar\gamma_{RF}}}\times\left(1-W\left(\gamma_{th}c\right)^{\frac{\xi^2-1}{2}}\frac{2^{1-\xi^2}}{\sqrt{\pi}}\left(\frac{k+1}{\bar\gamma_{RF}}\right)^{\frac{1-\xi^2}{2}}\times G_{4,7}^{5,2}\left(\frac{\lambda^2c(k+1)\gamma_{th}}{4A_0^2\bar\gamma_{FSO}\bar\gamma_{RF}}\middle|\begin{matrix}\varphi_1\\ \varphi_2\end{matrix}\right)\right)\left[1-\left(1-e^{-\frac{\gamma_{th}}{\bar\gamma_{RF}}}\right)W\gamma_{th}^{\frac{\xi^2-1}{2}}\times G_{2,3}^{2,1}\left(\frac{\lambda}{A_0}\sqrt{\frac{\gamma_{th}}{\bar\gamma_{FSO}}}\middle|\begin{matrix}1-\xi^2,1\\ 0,2-\xi^2,-\xi^2\end{matrix}\right)\right]^{M-1}. \tag{37}$$

Substituting binomial expansion of $\left[1-\left(1-e^{-\frac{\gamma_{th}}{\bar\gamma_{RF}}}\right)W\gamma_{th}^{\frac{\xi^2-1}{2}}\times G_{2,3}^{2,1}\left(\frac{\lambda}{A_0}\sqrt{\frac{\gamma_{th}}{\bar\gamma_{FSO}}}\middle|\begin{matrix}1-\xi^2,1\\ 0,2-\xi^2,-\xi^2\end{matrix}\right)\right]^{M-1}$ as $\sum_{t=0}^{M-1}\sum_{u=0}^{t}\binom{M-1}{t}\binom{t}{u}(-1)^{t+u}e^{-\frac{u\gamma_{th}}{\bar\gamma_{RF}}}\left(W\gamma_{th}^{\frac{\xi^2-1}{2}}\times G_{2,3}^{2,1}\left(\frac{\lambda}{A_0}\sqrt{\frac{\gamma_{th}}{\bar\gamma_{FSO}}}\middle|\begin{matrix}1-\xi^2,1\\ 0,2-\xi^2,-\xi^2\end{matrix}\right)\right)^t$, Outage Probability of the proposed structure in Negative Exponential atmospheric turbulence with the effect of pointing error becomes equal to:

$$P_{out}\left(\gamma_{th}\right)=1-\sum_{k=0}^{N-1}\sum_{t=0}^{M-1}\sum_{u=0}^{t}\Omega_4 e^{-\frac{(k+u+1)\gamma_{th}}{\bar\gamma_{RF}}}\times\left(1-W\left(\gamma_{th}c\right)^{\frac{\xi^2-1}{2}}\frac{2^{1-\xi^2}}{\sqrt{\pi}}\left(\frac{k+1}{\bar\gamma_{RF}}\right)^{\frac{1-\xi^2}{2}}\times G_{4,7}^{5,2}\left(\frac{\lambda^2c(k+1)\gamma_{th}}{4A_0^2\bar\gamma_{FSO}\bar\gamma_{RF}}\middle|\begin{matrix}\varphi_1\\ \varphi_2\end{matrix}\right)\right)\times\left(W\gamma_{th}^{\frac{\xi^2-1}{2}}G_{2,3}^{2,1}\left(\frac{\lambda}{A_0}\sqrt{\frac{\gamma_{th}}{\bar\gamma_{FSO}}}\middle|\begin{matrix}1-\xi^2,1\\ 0,2-\xi^2,-\xi^2\end{matrix}\right)\right)^t. \tag{38}$$

where $\Omega_4=\binom{N-1}{k}\binom{M-1}{t}\binom{t}{u}(-1)^{k+t+u}\frac{N}{k+1}$.

4.2. BER

Substituting (35) into (24), BER of DBPSK modulation in Gamma–Gamma atmospheric turbulence with the effect of pointing error becomes equal to:

$$P_e=\frac{1}{2}\int_0^\infty e^{-\gamma}\left\{1-\sum_{k=0}^{N-1}\sum_{t=0}^{M-1}\sum_{u=0}^{t}\Omega_3 e^{-\frac{(k+u+1)\gamma}{\bar\gamma_{RF}}}\left(\frac{\xi^2}{\Gamma(\alpha)\Gamma(\beta)}\times G_{2,4}^{3,1}\left(\alpha\beta\kappa\sqrt{\frac{\gamma}{\bar\gamma_{FSO}}}\middle|\begin{matrix}1,\xi^2+1\\ \xi^2,\alpha,\beta,0\end{matrix}\right)\right)^t\left[1-\frac{\xi^2 2^{\alpha+\beta-3}}{\pi\Gamma(\alpha)\Gamma(\beta)}\times G_{4,9}^{7,2}\left(\frac{(\alpha\beta\kappa)^2C(k+1)\gamma}{16\bar\gamma_{FSO}\bar\gamma_{RF}}\middle|\begin{matrix}\psi_1\\ \psi_2\end{matrix}\right)\right]\right\}d\gamma. \tag{39}$$

When $t>1$, because of the multiplication of three Meijer-G functions and one exponential function, the above integral is unsolvable. In the following, exact and asymptotic expressions are derived for BER of the proposed system in Gamma–Gamma atmospheric turbulence with the effect of pointing error.

Substituting (53) from Appendix B, into (35) leads to a new form of Outage Probability for the proposed structure; substituting the result into (24) and using [37, Eq. 07.34.21.0088.01], exact BER of DBPSK modulation in Gamma–Gamma atmospheric turbulence with the effect of pointing error becomes equal to:

$$P_e=\frac{1}{2}\left\{1+\sum_{k=0}^{N-1}\sum_{t=0}^{M-1}\sum_{u=0}^{t}\sum_{k_1=0}^{t}\sum_{k_2=0}^{k_1}\sum_{n=0}^{\infty}\Omega_3\binom{t}{k_1}\binom{k_1}{k_2}X_0^{t-k_1}\left(Y_n^{(k_1-k_2)} *Z_n^{(k_2)}\right)\frac{\left(\frac{1}{\bar\gamma_{FSO}}\right)^{\aleph}}{\left(1+\frac{k+u+1}{\bar\gamma_{RF}}\right)^{1+\aleph}}\left[\Gamma(1+\aleph)-\frac{\xi^2 2^{\alpha+\beta-3}}{\pi\Gamma(\alpha)\Gamma(\beta)}\times G_{5,9}^{7,3}\left(\frac{(\alpha\beta\kappa)^2C(k+1)}{16\bar\gamma_{FSO}\left(\bar\gamma_{RF}+k+u+1\right)}\middle|\begin{matrix}-\aleph,\psi_1\\ \psi_2\end{matrix}\right)\right]\right\}. \tag{40}$$

Substituting (56) from Appendix C into (35) leads to asymptotic Outage Probability for the proposed structure; substituting the result into (24) and using [37, Eq. 07.34.21.0088.01], asymptotic BER of DBPSK modulation in Gamma–Gamma atmospheric turbulence with the effect of pointing error becomes equal to:

$$P_e\cong\frac{1}{2}\left\{1-\sum_{k=0}^{N-1}\sum_{t=0}^{M-1}\sum_{u=0}^{t}\frac{\Omega_3(\Xi)^t}{\left(1+\frac{k+u+1}{\bar\gamma_{RF}}\right)^{\frac{Ot}{2}+1}}\left[\Gamma\left(\frac{Ot}{2}+1\right)-\frac{\xi^2 2^{\alpha+\beta-3}}{\pi\Gamma(\alpha)\Gamma(\beta)}G_{5,9}^{7,3}\left(\frac{(\alpha\beta\kappa)^2C(k+1)}{16\bar\gamma_{FSO}\left(\bar\gamma_{RF}+k+u+1\right)}\middle|\begin{matrix}-\frac{Ot}{2},\psi_1\\ \psi_2\end{matrix}\right)\right]\right\}. \tag{41}$$

Substituting (38) into (24) BER of DBPSK modulation in Negative Exponential atmospheric turbulence with the effect of pointing error becomes equal to:

$$P_e=\frac{1}{2}\int_0^\infty e^{-\gamma}\left\{1-\sum_{k=0}^{N-1}\sum_{t=0}^{M-1}\sum_{u=0}^{t}\Omega_4 e^{-\frac{(k+u+1)\gamma}{\bar\gamma_{RF}}}\times\left(1-W(\gamma c)^{\frac{\xi^2-1}{2}}\frac{2^{1-\xi^2}}{\sqrt{\pi}}\left(\frac{k+1}{\bar\gamma_{RF}}\right)^{\frac{1-\xi^2}{2}}\times G_{4,7}^{5,2}\left(\frac{\lambda^2c(k+1)\gamma}{4A_0^2\bar\gamma_{FSO}\bar\gamma_{RF}}\middle|\begin{matrix}\varphi_1\\ \varphi_2\end{matrix}\right)\right)\times\left(W\gamma^{\frac{\xi^2-1}{2}}G_{2,3}^{2,1}\left(\frac{\lambda}{A_0}\sqrt{\frac{\gamma}{\bar\gamma_{FSO}}}\middle|\begin{matrix}1-\xi^2,1\\ 0,2-\xi^2,-\xi^2\end{matrix}\right)\right)^t\right\}d\gamma. \tag{42}$$

Table 1
Constants used in simulation.

Constant	Definition
N	Number of users
M	Number of relays
η	Optical conversion efficiency
γ_{avg}	Electrical average SNR
γ_{th}	Electrical threshold SNR
α	Parameter related to atmospheric turbulence intensity
β	Parameter related to atmospheric turbulence intensity
ξ	Parameter related to pointing Error intensity
C	Fixed gain constant

When $t > 1$, because of the multiplication of three Meijer-G and one exponential functions, the above integral is unsolvable. In the following, a new exact expression is derived for BER of the proposed structure in Negative Exponential atmospheric turbulence with the effect of pointing error.

Substituting (60) from Appendix D into (38) leads to a new form of Outage Probability for the proposed structure; substituting the result into (24) and using [37, Eq. 07.34.21.0088.01], exact BER of DBPSK modulation in Negative Exponential atmospheric turbulence with the effect of pointing error becomes equal to:

$$P_e = \frac{1}{2}\left\{1 - \sum_{k=0}^{N-1}\sum_{t=0}^{M-1}\sum_{u=0}^{t}\sum_{k1=0}^{t}\sum_{n=0}^{\infty}\Omega_4 F_0^{t-k1} E_n^{(k_1)}\left(\frac{\Gamma(H+1)}{\left(1+\frac{k+u+1}{\bar{\gamma}_{RF}}\right)^{1+H}} - \frac{2^{1-\xi^2}}{\sqrt{\pi}} W\left(\frac{\bar{\gamma}_{RF}}{k+1}\right)^{\frac{1-\xi^2}{2}} \frac{c^{\xi^2-1}}{\left(1+\frac{k+u+1}{\bar{\gamma}_{RF}}\right)^{H}} \times G_{5,7}^{5,3}\left(\frac{\lambda^2 c(k+1)}{4A_0^2\bar{\gamma}_{FSO}(\bar{\gamma}_{RF}+k+u+1)}\middle|\begin{matrix}-H,\varphi_1\\ \varphi_2\end{matrix}\right)\right)\right\}. \quad (43)$$

5. Simulation results

This section discusses and compares analytical and simulation results for the performance evaluation of the proposed structure. Performance of the proposed structure is investigated for different number of users (N) and number of relays (M) for both cases of known and unknown CSI. The FSO link, in moderate to strong and in saturated atmospheric turbulence regimes is respectively modeled by Gamma–Gamma and Negative Exponential distributions. In order to get closer to the actual results, the effect of pointing error is also considered. Radial displacement of pointing error is assumed to have zero mean and is modeled by Rayleigh distribution. The RF link is considered to have fading with Rayleigh distribution. For simplicity and without loss of generality, FSO and RF links are assumed to have equal average SNR ($\bar{\gamma}_{FSO} = \bar{\gamma}_{RF} = \gamma_{avg}$). In addition, it is assumed that $\eta = 1$, $A_0 = 1$, and $C = 1$. Moderate ($\alpha = 4, \beta = 1.9, \xi = 10.45$) and strong ($\alpha = 4.2, \beta = 1.4, \xi = 2.45$) regimes of Gamma–Gamma atmospheric turbulence with the effect of pointing error are considered. Outage threshold SNR of the proposed system is represented by γ_{th} (see Table 1).

In MATLAB simulations, Gamma–Gamma random variable can be generated by multiplication of two Gamma random variable using *gamrnd(.)* command. Negative Exponential random variable can be generated using *exprnd(.)* command. Radial displacement of pointing error can be generated by complex addition of two Gaussian random variables using *randn(.)* command. In simulations, first 10^6 DBPSK data samples are generated; the other parts of the simulation including data transmission, reception, selection, amplification or demodulation, etc, are done exactly based on the descriptions of Section 2 (see Fig. 1).

In Fig. 2, Outage Probability of the proposed structure is plotted as a function of average SNR for a various number of relays, for both cases of known CSI and unknown CSI, at the moderate regime of Gamma–Gamma atmospheric turbulence with the effect of pointing error, when the number of users is $N = 2$ and threshold SNR is $\gamma_{th} = 10$ dB. When CSI is known, using different numbers of relays shows different performances at low γ_{avg}, but while increasing γ_{avg} this difference tends to disappear. Also, increasing number of relays does not have effect on the performance of the proposed structure. In the sense that, it can show an appropriate performance even at the long-range links. It can be seen that in the case of unknown CSI that system performance depends considerably on the number of relays. At low target Outage Probability, γ_{avg} difference between using different numbers of relays is more. For example, at $P_{out} = 10^{-2}$, γ_{avg} difference between $M = 1$ and $M = 2$ is 2 dB, and between $M = 1$ and $M = 3$ is 4 dB. At $P_{out} = 10^{-4}$, these differences are 2.5 dB and 5 dB, respectively.

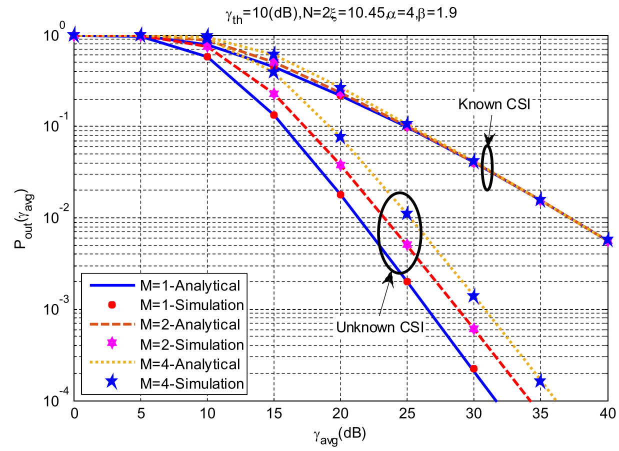

Fig. 2. Outage Probability of the proposed structure as a function of average SNR for various number of relays, and both cases of known CSI and unknown CSI, at moderate regime of Gamma–Gamma atmospheric turbulence with the effect of pointing error, when number of users is $N = 2$ and $\gamma_{th} = 10$ dB.

An important subject to discuss is the outperforming of unknown CSI compared with known CSI scheme. At equal power consumptions, the known CSI scheme should perform better than unknown CSI. Because when CSI is known, the relay adjusts its amplification gain according to conditions, but in unknown CSI case, the amplification gain is fixed at all conditions. However, this statement is not generally correct when there is no constraint (e.g. equality) on transmitted power. As can be seen in (6), there is a desired constant parameter (C) in the amplification gain of unknown CSI scheme. Therefore, the amplification gain of unknown CSI scheme could be adjusted manually. In simulations of this paper, this gain is adjusted so that to have good performance at all SNR ranges. That is why the fixed gain scheme outperforms variable gain scheme. It can be concluded that the larger amplification gain, the higher outperform of unknown CSI compared with known CSI scheme.

In Fig. 3, BER of the proposed structure is plotted as a function of average SNR for a various number of users, for both cases of known CSI and unknown CSI, at the moderate regime of Gamma–Gamma atmospheric turbulence with the effect of pointing error, when number of relays is $M = 2$. One of the main advantages of the proposed structure is its low dependence on the number of users in both cases of known and unknown CSI. In the proposed structure, the access point selects the user with the maximum SNR. Different users encounter independent fading; therefore, the probability of finding a user with favorable channel condition increases while increasing number of users. As can be seen, the performance in the case of $N = 5$ is better than $N = 2$. At high γ_{avg}, system sensitivity to the number of users decreases, i.e. the system performs almost independent of the number of users. Therefore, the proposed structure is suitable for areas with variable population density. Also, it has worth mentioning that this

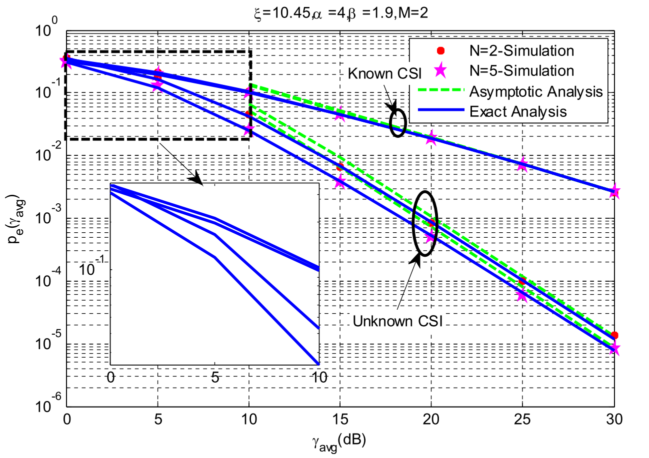

Fig. 3. Bit Error Rate of the proposed structure as a function of average SNR for various number of users, and both cases of known CSI and unknown CSI, at moderate regime of Gamma–Gamma atmospheric turbulence with the effect of pointing error when number of relays is $M = 2$.

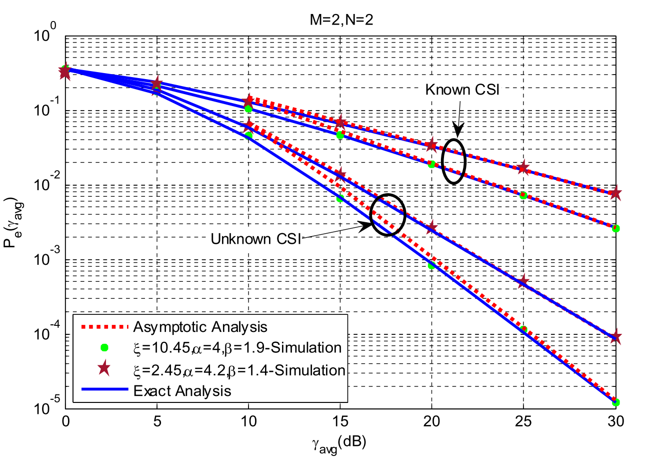

Fig. 4. Bit Error Rate of the proposed structure as a function of average SNR, and both cases of known CSI and unknown CSI, at moderate and strong regimes of Gamma–Gamma atmospheric turbulence with the effect of pointing error when number of relays is $M = 2$ and number of users is $N = 2$.

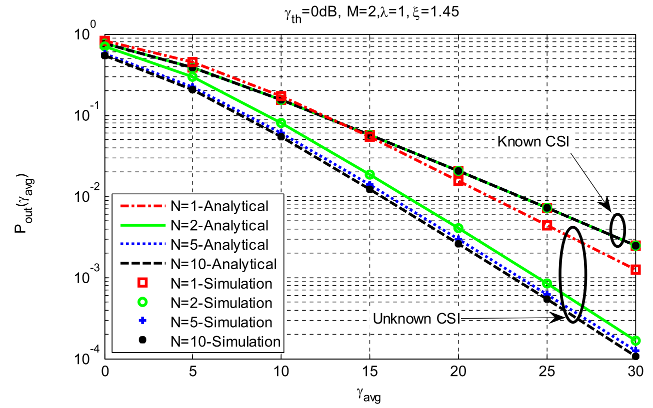

Fig. 5. Outage Probability of the proposed structure as a function of average SNR for various number of users, and both cases of known CSI and unknown CSI, at Negative Exponential atmospheric turbulence with the effect of pointing error with unit variance, when number of relay is $M = 2$, $\xi = 1.45$, and $\gamma_{th} = 10$ dB.

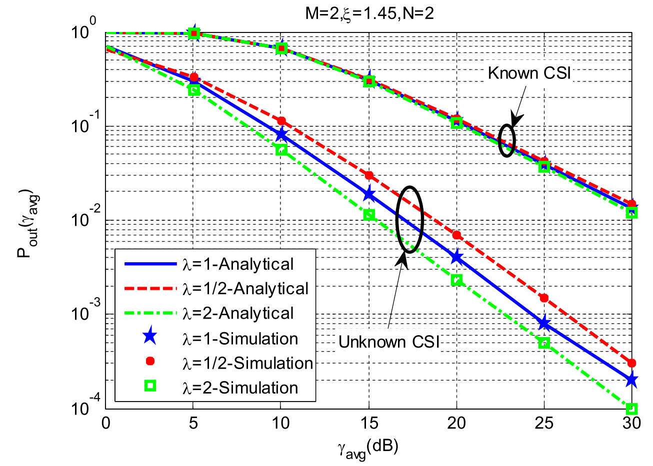

Fig. 6. Outage Probability of the proposed structure as a function of average SNR for various variances of Negative Exponential atmospheric turbulence with the effect of pointing error, and both cases of known CSI and unknown CSI, when number of relays is $M = 2$ and number of users is $N = 2$, and $\xi = 1.45$.

independent performance is achieved without additional complexity or processing. The performance of unknown CSI is a bit more dependent on the number of users than performance of known CSI. Because when CSI is known, the amplification gain is adjusted adaptively, but in the other case, the amplification gain remains fixed in all scenarios. Known CSI scheme has more complexity but reliability in data transmission.

In Fig. 4, BER of the proposed structure is plotted as a function of average SNR, for both cases of known CSI and unknown CSI, at moderate and strong regimes of Gamma–Gamma atmospheric turbulence with the effect of pointing error when the number of relays is $M = 2$ and number of users is $N = 2$. Another advantage of the proposed structure is its independent performance at different atmospheric turbulence regimes. Results indicate that at low γ_{avg}, system performance at moderate and strong atmospheric turbulence has low difference. Therefore, there is no need to add processing or consume power in order to maintain the performance at different atmospheric turbulence regimes. Accordingly, this structure is significantly recommended for mobile communication systems in which power consumption and processing complexity are two important factors. In this paper, the asymptotic analysis is done due to the high computational complexity of obtained exact expressions. As can be seen, obtained asymptotic and exact analysis match properly at high γ_{avg}.

In Fig. 5, Outage Probability of the proposed structure is plotted as a function of average SNR for various number of users, and both cases of known CSI and unknown CSI, at Negative Exponential atmospheric turbulence with the effect of pointing error with unit variance, when number of relays is $M = 2$, $\xi = 1.45$, and $\gamma_{th} = 10$ dB. In saturated regime, the same as moderate and strong regime, the proposed structure performs almost independent at different population densities. This independence is a bit more in known CSI scheme. In dense populations, it is more likely to find a signal with desirable γ_{avg}; therefore, the system performs better in this case.

In Fig. 6, Outage Probability of the proposed structure is plotted as a function of average SNR for various variances of Negative Exponential atmospheric turbulence with the effect of pointing error, and both cases of known CSI and unknown CSI, when the number of relays is $M = 2$ and number of users is $N = 2$, and $\xi = 1.45$. Again, the outperformance of unknown CSI scheme can be observed here. This is because when CSI is unknown, the amplification gain is fixed and adjusted manually; usually, operators define this gain according to the worst-case scenario and that is exactly why this scheme performs better than known CSI scheme. In spite of more power consumption of unknown CSI scheme, it has less complexity and processing and is especially suitable for communication systems with timing or performance demand.

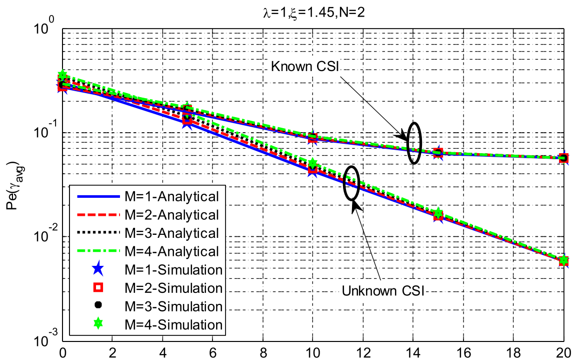

Fig. 7. Bit Error Rate of the proposed structure as a function of average SNR for various number of relays, and both cases of known CSI and unknown CSI, at Negative Exponential atmospheric turbulence with the effect of pointing error with unit variance, when number of users is $N = 2$, and $\xi = 1.45$.

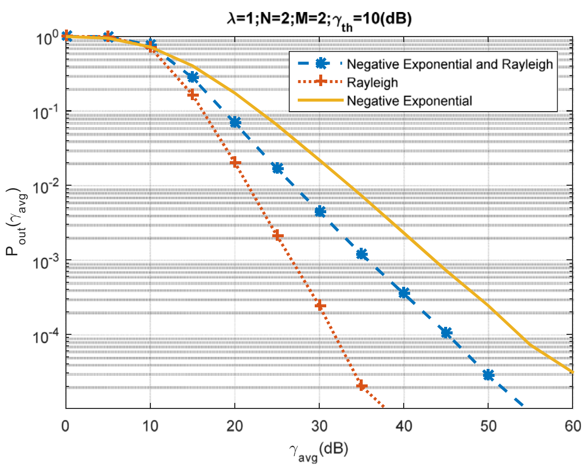

Fig. 8. Outage Probability of the proposed structure as a function of average SNR for various channel model scenarios, at unit variance of Negative Exponential atmospheric turbulence, when CSI is unknown, the number of relays is $M = 2$ and number of users is $N = 2$.

In Fig. 7, BER of the proposed structure is plotted as a function of average SNR for a various number of relays, and both cases of known CSI and unknown CSI, at Negative Exponential atmospheric turbulence with the effect of pointing error with unit variance, when the number of users is $N = 2$, and $\xi = 1.45$. As can be seen, in both cases of known CSI and unknown CSI, at low γ_{avg}, there is a slight performance difference between different number of relays, and this difference is a bit more in the case of unknown CSI. In both cases of known CSI and unknown CSI, at high γ_{avg}, system performance is independent of the number of relays. Generally speaking, series relaying structure degrades system performance, because of frequent decisions made by relays.

Figs. 8 and 9 are conducted to have more investigation on the proposed structure. In Fig. 8, the outage probability of the proposed structure is investigated at three different channel model scenarios. The first scenario is the proposed channel model scenario of this paper (noting changed; Rayleigh fading and Negative Exponential atmospheric turbulence); in the second scenario, it is assumed that all of the transmitters of the proposed structure are RF transmitters and there is no FSO transmitter in the system (actually the FSO transmitters are replaced by RF transmitters; the fading is Rayleigh). The third scenario assumes that all of transmitters are FSO (RF transmitters are replaced by FSO; the atmospheric turbulence is Negative Exponential). Other general assumptions are unknown CSI scheme, number of relays is $M = 2$ and number of users is $N = 2$. As can be expected, the second case performs better than the first case and the first case performs better than the first case. This is because the strength of Negative Exponential atmospheric turbulence is more than the Rayleigh fading. Although the proposed structure (first scenario) does not perform better than the second scenario, it should be considered that the main propose of presenting this structure was the problem of long-range links and impassable areas where RF connection disrupts easily. Actually, one of the natural properties of the hybrid FSO/RF systems is their complementary, and this property could help to solve this problem.

In order to have more insights into the advantages or disadvantages of this work, the proposed structure should be compared with the most similar works. Actually, there are many works in FSO or RF, but generally, in order to compare two things, they should have at least some similarities. [18], and [21] has presented the most similar structures to this work (they clearly plotted their proposed structures). They are both dual hop, at the first hop a multi-user communication is developed and users want to connect to an access point; at the second hop, either an FSO or a parallel FSO/RF link connects the access point to the Base Station. So these structures are the best for comparing with. Fig. 9. Plots the BER and Outage Probability of the proposed structure, [18], and [21], as functions of average SNR, at unit variance of Negative Exponential atmospheric turbulence, when CSI is unknown, the number of relays is $M = 2$ and number of users is $N = 2$. As can be seen, [18] performs better than [21] and the proposed structure; this is because [18] has a parallel FSO/RF link at its second hop. It is proven that parallel FSO/RF links could greatly improve the performance of the system because there is almost no condition under which both FSO and RF links get disrupted. Also, it can be seen that [21] performs better than the proposed structure. This is because the proposed structure has more hops ($M = 2$) and as discussed before, increasing the hops number decreases the performance. Because by increasing number of hops number of decisions made on the signal (detections) increases and this degrades the performance. The main disadvantage of multi-hop structures is the reduction in performance due to multiple decisions on the signal.

The performance is not all of the things that should be considered; it should be considered that why the proposed structure is presented. In this paper there was no discussion about the performance of the system; the three main factors for selecting different parts of the proposed structure are processing, power consumption, and the cost. Also, simulation results indicate that the proposed structure is a good choice for the problem of long-range impassable areas. Generally speaking, there are two ways for solving the problem of long-range impassable areas: increasing the transmission power, and multi-hop communication; the second way is the efficient way. None of the compared structures in Figs. 8 and 9, despite their performance, could not be preferable in such case. As results show, the main advantage of the proposed structure is the maintenance of its properties in a wide range of atmospheric turbulence regimes from moderate to saturated. Results indicate that properties such as low dependence on number of users, number of relays, as well as atmospheric turbulence intensity, could be achieved at any turbulence regime. This is because of the nature of the hybrid FSO/RF systems; they are naturally reliable and accessible.

Concluding the results, this structure verified that even in the worth case scenario (long-range impassable area under saturated atmospheric turbulence with the effect of pointing error) it is possible to have a reliable favorite communication by simply use of some relays and FSO/RF transmitters. Simplicity is something forgotten in modern communication systems. But this paper by considering power, processing, and cost, selected and combined some quite simple schemes such as multi-user communication, signal selection at each relay station, multi-hop relaying, and finally achieved some advantages which in modern communication systems should bring heavy processing, cost or power consumption to deserve them.

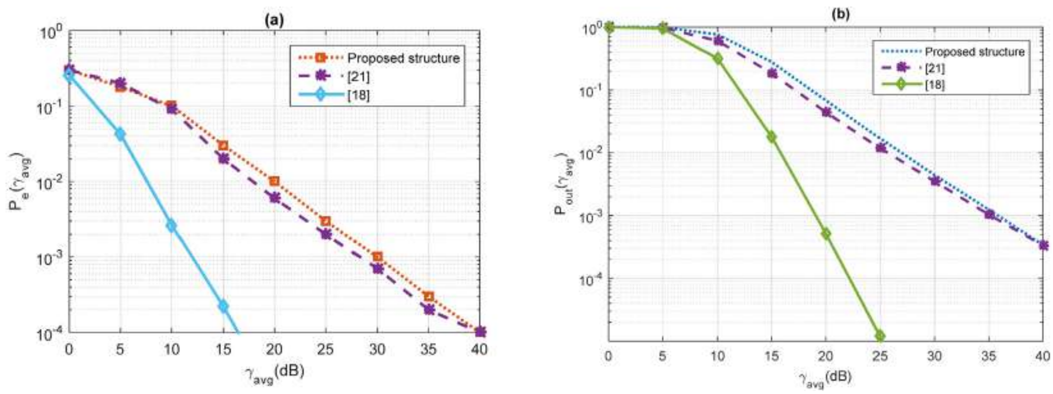

Fig. 9. BER and Outage Probability of the proposed structure, [18], and [21], as a function of average SNR, at unit variance of Negative Exponential atmospheric turbulence, when CSI is unknown, the number of relays is $M = 2$ and number of users is $N = 2$.

6. Conclusion

In this paper, a novel multi-user multi-hop hybrid FSO/RF communication system is presented, which is consisted of two main parts. In the first part, an access point connects the RF users to the source Base Station via a series dual hop hybrid FSO/RF link. In the second part, a multi-hop parallel hybrid FSO/RF link connects source and destination Base Stations. This structure is suitable for impassable areas or long-range links that direct RF connection between mobile users and the source Base Station is not possible. The FSO link in moderate to strong and in saturated atmospheric turbulence regimes is respectively modeled by Gamma–Gamma and Negative Exponential distributions. In order to get closer to the actual results, the effect of pointing error is also considered. Fading of the RF link has Rayleigh distribution. New expressions are derived for BER and Outage Probability of the proposed structure and verified via MATLAB simulations. Two cases of CSI existence and non-existence at the access point are investigated at a various number of users and relays. One of the observed advantages of the proposed structure is its low dependence on the number of users; therefore, it is suitable for areas with variable population density. Another advantage is the maintenance of the performance at a wide range of atmospheric turbulence, which proves the reliability of the proposed structure. Also results confirmed low dependence on the number of relays; hence it is a good choice for long-range links. In simulation results, unknown CSI outperformed known CSI, this is because when CSI is unknown, the amplification gain is fixed and chosen manually. In this paper, this gain is defined according to the worst-case scenario and that is exactly why this scheme performs better than the known CSI scheme.

Appendix A. The CDF of negative exponential atmospheric turbulence with the effect of pointing error

The marginal pdf of pointing error and Negative Exponential atmospheric turbulence are respectively as follows [8]:

$$f_{h_p}\left(h_p\right) = \frac{\xi^2}{A_0^{\xi^2}} h_p^{\xi^2-1}; 0 \le h_p \le A_0, \tag{44}$$

$$f_{h_a}\left(h_a\right) = \lambda e^{-\lambda h_a} \tag{45}$$

where $1/\lambda^2$ is Negative Exponential atmospheric turbulence variance, $A_0 = [\mathrm{erf}(v)]^2$, $v = \sqrt{\pi/2}R/w_b$, R is the radius of the receiver aperture, w_b is the received beam size. The joint pdf of Negative Exponential atmospheric turbulence and the pointing error effect can be calculated as follows:

$$f_{\mathrm{h}}(h) = \int_{\frac{\mathrm{h}}{\mathrm{A}_0}}^{\infty} f_{h_a}\left(\frac{h}{h_a}\middle| h_a\right) f_{h_a}\left(h_a\right) dh_a$$

$$= \int_{\frac{\mathrm{h}}{\mathrm{A}_0}}^{\infty} \frac{\xi^2}{A_0^{\xi^2}} \left(\frac{h}{h_a}\right)^{\xi^2-1} \lambda e^{-\lambda h_a} dh_a \tag{46}$$

$$= \frac{\xi^2 \lambda^{\xi^2-1}}{A_0^{\xi^2}} h^{\xi^2-1} \Gamma\left(2-\xi^2, \frac{\lambda \mathrm{h}}{\mathrm{A}_0}\right).$$

According that $\gamma = \bar{\gamma}_{FSO} h^2$, and using equivalent Meijer-G form of $\Gamma\left(2-\xi^2, \frac{\lambda}{\mathrm{A}_0}\sqrt{\frac{\gamma}{\bar{\gamma}_{FSO}}}\right)$ as $G_{1,2}^{2,0}\left(\frac{\lambda}{\mathrm{A}_0}\sqrt{\frac{\gamma}{\bar{\gamma}_{FSO}}}\middle| \begin{matrix} 1-\xi^2, 1 \\ 0, 2-\xi^2, -\xi^2 \end{matrix}\right)$, the pdf of Negative Exponential atmospheric turbulence with the effect of pointing error becomes equal to:

$$f_{\gamma_{\mathrm{FSO}}}(\gamma) = W \gamma^{\frac{\xi^2}{2}-1} G_{1,2}^{2,0}\left(\frac{\lambda}{A_0}\sqrt{\frac{\gamma}{\bar{\gamma}_{FSO}}}\middle| \begin{matrix} 1 \\ 0, 2-\xi^2 \end{matrix}\right), \tag{47}$$

where $W = \frac{\xi^2 \lambda^{\xi^2-1}}{2A_0^{\xi^2} \bar{\gamma}_{FSO}^{\xi^2/2}}$. Integrating (47), the CDF of Negative Exponential atmospheric turbulence with the effect of pointing error becomes as follows:

$$F_{\gamma_{\mathrm{FSO}}}(\gamma) = W \gamma^{\frac{\xi^2-1}{2}} G_{2,3}^{2,1}\left(\frac{\lambda}{A_0}\sqrt{\frac{\gamma}{\bar{\gamma}_{FSO}}}\middle| \begin{matrix} 1-\xi^2, 1 \\ 0, 2-\xi^2, -\xi^2 \end{matrix}\right). \tag{48}$$

Appendix B. Exact CDF of Gamma–Gamma atmospheric turbulence considering the effect of pointing error

Using [37, Eq. 07.34.26.0004.01], the pdf of Gamma–Gamma atmospheric turbulence with the effect of pointing error is equal to:

$$\begin{aligned} f_{\gamma_{FSO}}(\gamma) = & \frac{\xi^2 \Gamma\left(\alpha-\xi^2\right) \Gamma\left(\beta-\xi^2\right)}{2\Gamma(\alpha)\Gamma(\beta)\gamma} \left(\alpha\beta\kappa\sqrt{\frac{\gamma}{\bar{\gamma}_{FSO}}}\right)^{\xi^2} \\ & \times {}_1F_2\left(0; 1-\alpha+\xi^2, 1-\beta+\xi^2; \alpha\beta\kappa\sqrt{\frac{\gamma}{\bar{\gamma}_{FSO}}}\right) \\ & + \frac{\xi^2 \Gamma\left(\xi^2-\alpha\right) \Gamma(\beta-\alpha)}{2\Gamma(\alpha)\Gamma(\beta)\Gamma\left(\xi^2+1-\alpha\right)\gamma} \left(\alpha\beta\kappa\sqrt{\frac{\gamma}{\bar{\gamma}_{FSO}}}\right)^{\alpha} \\ & \times {}_1F_2\left(\alpha-\xi^2; 1-\xi^2+\alpha, 1-\beta+\alpha; \alpha\beta\kappa\sqrt{\frac{\gamma}{\bar{\gamma}_{FSO}}}\right) \\ & + \frac{\xi^2 \Gamma(\alpha-\beta) \Gamma\left(\xi^2-\beta\right)}{2\Gamma(\alpha)\Gamma(\beta)\Gamma\left(\xi^2+1-\beta\right)\gamma} \left(\alpha\beta\kappa\sqrt{\frac{\gamma}{\bar{\gamma}_{FSO}}}\right)^{\beta} \\ & \times {}_1F_2\left(\beta-\xi^2; 1-\xi^2+\beta, 1-\alpha+\beta; \alpha\beta\kappa\sqrt{\frac{\gamma}{\bar{\gamma}_{FSO}}}\right) \end{aligned} \tag{49}$$

where ${}_pF_q\left(a_1, \dots, a_p; b_1, \dots, b_q; z\right)$ is the Hyper-geometric function [37, Eq. 07.31.02.0001.01]. Using [37, Eq. 07.23.02.0001.01], the above expression becomes equal to:

$$f_{\gamma_{FSO}}(\gamma) = \frac{\xi^2}{2\bar{\gamma}_{FSO}} X_0 \left(\frac{\gamma}{\bar{\gamma}_{FSO}}\right)^{\frac{\xi^2}{2}-1} + \sum_{n=0}^{\infty} \frac{n+\alpha}{2\bar{\gamma}_{FSO}} Y_n \left(\frac{\gamma}{\bar{\gamma}_{FSO}}\right)^{\frac{n+\alpha}{2}-1}$$

$$+\sum_{n=0}^{\infty}\frac{n+\beta}{2\bar{\gamma}_{FSO}}Z_n\left(\frac{\gamma}{\bar{\gamma}_{FSO}}\right)^{\frac{n+\beta}{2}-1}, \tag{50}$$

where $X_0=\frac{\Gamma\left(\alpha-\xi^2\right)\Gamma\left(\beta-\xi^2\right)}{\Gamma(\alpha)\Gamma(\beta)}(\alpha\beta\kappa)^{\xi^2}$,

$Y_n=\frac{\xi^2\Gamma\left(\xi^2-\alpha\right)\Gamma(\beta-\alpha)\left(\alpha-\xi^2\right)_n}{(n+\alpha)\Gamma(\alpha)\Gamma(\beta)\Gamma\left(\xi^2+1-\alpha\right)\left(1-\xi^2+\alpha\right)_n(1-\beta+\alpha)_n n!}(\alpha\beta\kappa)^{n+\alpha}$,

and $Z_n=\frac{\xi^2\Gamma(\alpha-\beta)\Gamma\left(\xi^2-\beta\right)\left(\beta-\xi^2\right)_n}{(n+\beta)\Gamma(\alpha)\Gamma(\beta)\Gamma\left(\xi^2+1-\beta\right)\left(1-\xi^2+\beta\right)_n(1-\alpha+\beta)_n n!}(\alpha\beta\kappa)^{n+\beta}$. Note that $(.)_n$ is the pochhammer symbol [39]. Integrating (50), the CDF of Gamma–Gamma atmospheric turbulence with the effect of pointing error becomes equal to[1]:

$$F_{\gamma_{FSO}}(\gamma)=X_0\left(\frac{\gamma}{\bar{\gamma}_{FSO}}\right)^{\frac{\xi^2}{2}}+\sum_{n=0}^{\infty}Y_n\left(\frac{\gamma}{\bar{\gamma}_{FSO}}\right)^{\frac{n+\alpha}{2}}+\sum_{n=0}^{\infty}Z_n\left(\frac{\gamma}{\bar{\gamma}_{FSO}}\right)^{\frac{n+\beta}{2}}. \tag{51}$$

Using (51), expression $\left(\frac{\xi^2}{\Gamma(\alpha)\Gamma(\beta)}G_{2,4}^{3,1}\left(\alpha\beta\kappa\sqrt{\frac{\gamma_{th}}{\bar{\gamma}_{FSO}}}\middle|\begin{matrix}1,\xi^2+1\\ \xi^2,\alpha,\beta,0\end{matrix}\right)\right)^t$ in (21) can be expanded by trinomial expansion as:

$$\sum_{k_1=0}^{t}\sum_{k_2=0}^{k_1}\binom{t}{k_1}\binom{k_1}{k_2}\left(X_0\left(\frac{\gamma_{th}}{\bar{\gamma}_{FSO}}\right)^{\frac{\xi^2}{2}}\right)^{t-k_1}\left(\sum_{n=0}^{\infty}Y_n\left(\frac{\gamma_{th}}{\bar{\gamma}_{FSO}}\right)^{\frac{n+\alpha}{2}}\right)^{k_1-k_2}$$
$$\times\left(\sum_{n=0}^{\infty}Z_n\left(\frac{\gamma_{th}}{\bar{\gamma}_{FSO}}\right)^{\frac{n+\beta}{2}}\right)^{k_2}, \tag{52}$$

after some mathematical simplification, it becomes as:

$$\sum_{k_1=0}^{t}\sum_{k_2=0}^{k_1}\sum_{n=0}^{\infty}\binom{t}{k_1}\binom{k_1}{k_2}X_0^{t-k_1}\left(Y_n^{(k_1-k_2)}*Z_n^{(k_2)}\right)\left(\frac{\gamma_{th}}{\bar{\gamma}_{FSO}}\right)^{\aleph}, \tag{53}$$

where $\aleph=\frac{n+\xi^2(t-k_1)+\alpha(k_1-k_2)+\beta k_2}{2}$, and (*) denotes the convolution and the subscript $h_n^{(k)}$ means that h_n is convolved (k-1) times with itself.

Appendix C. Asymptotic CDF of Gamma–Gamma atmospheric turbulence considering the effect of pointing error

Using approximation of [37, Eq. 07.34.06.0006.01], the asymptotic pdf of Gamma–Gamma atmospheric turbulence with the effect of pointing error becomes equal to:

$$f_{\gamma_{FSO}}(\gamma)\cong\begin{cases}\frac{\xi^2\Gamma(\alpha-\beta)\Gamma\left(\xi^2-\beta\right)}{2\Gamma(\alpha)\Gamma(\beta)\Gamma\left(\xi^2+1-\beta\right)\gamma}\left(\alpha\beta\kappa\sqrt{\frac{\gamma}{\bar{\gamma}_{FSO}}}\right)^{\beta} & \xi^2>\beta,\alpha>\beta\\ \frac{\xi^2\Gamma\left(\beta-\xi^2\right)\Gamma\left(\alpha-\xi^2\right)}{2\Gamma(\alpha)\Gamma(\beta)\gamma}\left(\alpha\beta\kappa\sqrt{\frac{\gamma}{\bar{\gamma}_{FSO}}}\right)^{\xi^2} & \alpha>\xi^2,\beta>\xi^2\\ \frac{\xi^2\Gamma\left(\xi^2-\alpha\right)\Gamma(\beta-\alpha)}{2\Gamma(\alpha)\Gamma(\beta)\Gamma\left(\xi^2+1-\alpha\right)\gamma}\left(\alpha\beta\kappa\sqrt{\frac{\gamma}{\bar{\gamma}_{FSO}}}\right)^{\alpha} & \beta>\alpha,\xi^2>\alpha\end{cases} \tag{54}$$

Integrating the above equation, the asymptotic CDF of Gamma–Gamma atmospheric turbulence with the effect of pointing error becomes as follows:

$$F_{\gamma_{FSO}}(\gamma)\cong\begin{cases}\frac{\xi^2\Gamma(\alpha-\beta)}{\Gamma(\alpha)\Gamma(\beta+1)\Gamma\left(\xi^2-\beta\right)}\left(\alpha\beta\kappa\sqrt{\frac{1}{\bar{\gamma}_{FSO}}}\right)^{\beta}\gamma^{\frac{\beta}{2}} & \xi^2>\beta,\alpha>\beta\\ \frac{\Gamma\left(\beta-\xi^2\right)\Gamma\left(\alpha-\xi^2\right)}{\Gamma(\alpha)\Gamma(\beta)}\left(\alpha\beta\kappa\sqrt{\frac{1}{\bar{\gamma}_{FSO}}}\right)^{\xi^2}\gamma^{\frac{\xi^2}{2}} & \alpha>\xi^2,\beta>\xi^2\\ \frac{\xi^2\Gamma(\beta-\alpha)}{\Gamma(\alpha+1)\Gamma(\beta)\Gamma\left(\xi^2-\alpha\right)}\left(\alpha\beta\kappa\sqrt{\frac{1}{\bar{\gamma}_{FSO}}}\right)^{\alpha}\gamma^{\frac{\alpha}{2}} & \beta>\alpha,\xi^2>\alpha\end{cases} \tag{55}$$

Which can be rewritten as:

$$F_{\gamma_{FSO}}(\gamma)\cong\Xi\gamma^{\frac{O}{2}}, \tag{56}$$

where

$$\begin{cases}\Xi=\frac{\xi^2\Gamma(\alpha-\beta)}{\Gamma(\alpha)\Gamma(\beta+1)\Gamma\left(\xi^2-\beta\right)}\left(\alpha\beta\kappa\sqrt{\frac{1}{\bar{\gamma}_{FSO}}}\right)^{\beta},O=\beta & \xi^2>\beta,\alpha>\beta\\ \Xi=\frac{\Gamma\left(\beta-\xi^2\right)\Gamma\left(\alpha-\xi^2\right)}{\Gamma(\alpha)\Gamma(\beta)}\left(\alpha\beta\kappa\sqrt{\frac{1}{\bar{\gamma}_{FSO}}}\right)^{\xi^2},O=\xi^2 & \alpha>\xi^2,\beta>\xi^2\\ \Xi=\frac{\xi^2\Gamma(\beta-\alpha)}{\Gamma(\alpha+1)\Gamma(\beta)\Gamma\left(\xi^2-\alpha\right)}\left(\alpha\beta\kappa\sqrt{\frac{1}{\bar{\gamma}_{FSO}}}\right)^{\alpha},O=\alpha & \beta>\alpha,\xi^2>\alpha.\end{cases}$$

Appendix D. Exact CDF of negative exponential atmospheric turbulence with the effect of pointing error

Using [37, Eq. 07.34.26.0004.01], the CDF of Negative Exponential atmospheric turbulence with the effect of pointing error is equal to:

$$F_{\gamma_{FSO}}(\gamma)=\frac{\Gamma\left(2-\xi^2\right)\Gamma\left(\xi^2\right)}{\Gamma\left(1+\xi^2\right)}{}_2F_2\left(\xi^2,0;\xi^2-1,\xi^2+1;-\frac{\lambda}{A_0}\sqrt{\frac{\gamma}{\bar{\gamma}_{FSO}}}\right) \tag{57}$$
$$+\frac{\Gamma\left(\xi^2-2\right)\Gamma(2)}{\Gamma\left(\xi^2-1\right)\Gamma(3)}\left(\frac{\lambda}{A_0}\sqrt{\frac{\gamma}{\bar{\gamma}_{FSO}}}\right)^{2-\xi^2}$$
$$\times{}_2F_2\left(2,2-\xi^2;3-\xi^2,3;-\frac{\lambda}{A_0}\sqrt{\frac{\gamma}{\bar{\gamma}_{FSO}}}\right)$$

Using [37, Eq. 07.23.02.0001.01], the above expression becomes equal to:

$$F_{\gamma_{FSO}}(\gamma)=F_0\gamma^{\frac{\xi^2-1}{2}}+\sum_{n=0}^{\infty}E_n\gamma^{\frac{n+1}{2}}, \tag{58}$$

where $F_0=\frac{\xi^2\lambda^{\xi^2-1}}{2A_0^{\xi^2}\bar{\gamma}_{FSO}^{\xi^2/2}}\frac{\Gamma\left(2-\xi^2\right)\Gamma\left(\xi^2\right)}{\Gamma\left(1+\xi^2\right)}$, and $E_n=\frac{\xi^2}{2}\frac{\Gamma\left(\xi^2-2\right)\Gamma(2)}{\Gamma\left(\xi^2-1\right)\Gamma(3)}\frac{(2)_n\left(2-\xi^2\right)_n(-1)^n}{(3)_n\left(3-\xi^2\right)_n n!}\frac{\lambda^{n+1}}{A_0^{n+2}}\frac{1}{\bar{\gamma}_{FSO}^{\frac{n+2}{2}}}$.

Using (58), expression $\left(W\gamma_{th}^{\frac{\xi^2-1}{2}}G_{2,3}^{2,1}\left(\frac{\lambda}{A_0}\sqrt{\frac{\gamma_{th}}{\bar{\gamma}_{FSO}}}\middle|\begin{matrix}1-\xi^2,1\\ 0,2-\xi^2,-\xi^2\end{matrix}\right)\right)^t$ in (21) can be expanded by trinomial expansion as:

$$\sum_{k_1=0}^{t}\binom{t}{k_1}\left(F_0\gamma_{th}\right)^{t-k_1}\left(\sum_{n=0}^{\infty}E_n\gamma_{th}^{\frac{n+1}{2}}\right)^{k_1}, \tag{59}$$

after some mathematical simplification, it becomes as:

$$\sum_{k_1=0}^{t}\sum_{n=0}^{\infty}\binom{t}{k_1}F_0^{t-k_1}E_n^{(k_1)}\gamma_{\mathrm{th}}^{H}, \tag{60}$$

where $H=\frac{n+\xi^2+k_1+(t-k_1)\left(\xi^2-1\right)}{2}$.

[1] The main idea of such transformation from Meijer-G to linear summation is taken from [39], Eqs. (10)–(14). In this paper, nontruncated value of n has revealed to show the convergence of the infinite series, because the use of a truncated value of n does not lead to an exact result, and "=" sign should be changed to "∼". But in MATLAB implementation code, n taken in (0,20) works.

References

[1] M.R. Bhatnagar, S. Anees, On the performance of Alamouti scheme in Gamma-Gamma fading FSO links with pointing errors, IEEE Wirel. Commun. Lett. 4 (1) (2015) 94–97.

[2] M.A. Esmail, H. Fathallah, M.S. Alouini, Outage probability analysis of FSO links over foggy channel, IEEE Photonics J. 9 (2) (2017) 1–12.

[3] W. Gappmair, H.E. Nistazakis, Subcarrier PSK performance in terrestrial FSO links impaired by gamma-gamma fading, pointing errors, and phase noise, J. Lightwave Technol. 35 (9) (2017) 1624–1632.
[4] P.K. Sharma, A. Bansal, P. Garg, T. Tsiftsis, R. Barrios, Relayed FSO communication with aperture averaging receivers and misalignment errors, IET Commun. 11 (1) (2017) 45–52.
[5] P.V. Trinh, T.C. Thang, A.T. Pham, Mixed mmwave RF/FSO relaying systems over generalized fading channels with pointing errors, IEEE Photonics J. 9 (1) (2017) 1–14.
[6] F.J. Lopez-Martinez, G. Gomez, J.M. Garrido-Balsells, Physical-layer security in free-space optical communications, IEEE Photonics J. 7 (2) (2015) 1–14.
[7] M.A. Amirabadi, V.T. Vakili, Performance analysis of hybrid FSO/RF communication systems with Alamouti Coding or Antenna Selection, arXiv preprint arXiv:1802.07286, (2018).
[8] M.A. Amirabadi, V.T. Vakili, A new optimization problem in the FSO communication system, IEEE Commun. Lett. 22 (7) (2018).
[9] L. Chen, W. Wang, C. Zhang, Multiuser diversity over parallel and hybrid FSO/RF links and its peRFormance analysis, IEEE Photon. J. 8 (3) (2016) 1–9.
[10] V.V. Mai, A.T. Pham, Adaptive multi-rate designs and analysis for hybrid fso/rf systems over fading channels, IEICE Trans. Commun. 98 (8) (2015) 1660–1671.
[11] M.N. Khan, M. Jamil, Adaptive hybrid free space optical/radio frequency communication system, Telecommun. Syst. 65 (1) (2017) 117–126.
[12] T. Rakia, H.C. Yang, F. Gebali, M.S. Alouini, Power adaptation based on truncated channel inversion for hybrid FSO/RF transmission with adaptive combining, IEEE Photonics J. 7 (4) (2015) 1–12.
[13] V.V. Mai, A.T. Pham, Adaptive multi-rate designs for hybrid fso/rf systems over fading channels, in: Globecom Workshops (GC Wkshps) 2014 IEEE, 2014, pp. 469–474.
[14] Z. Kolka, Z. Kincl, V. Biolkova, D. Biolek, Hybrid FSO/RF test link, in: Ultra Modern Telecommunications and Control Systems and Workshops (ICUMT), 2012 4th International Congress on, 2012, pp. 502–505.
[15] A. AbdulHussein, A. Oka, T.T. Nguyen, L. Lampe, Rateless coding for hybrid free-space optical and radio-frequency communication, IEEE Trans. Wirel. Commun. 9 (3) (2010).
[16] W. Zhang, S. Hranilovic, C. Shi, Soft-switching hybrid FSO/RF links using short-length raptor codes: design and implementation, IEEE J. Sel Areas Commun. 27 (9) (2009).
[17] M.A. Amirabadi, V.T. Vakili, A novel hybrid FSO/RF communication system with receive diversity, arXiv preprint arXiv:1802.07348, (2018).
[18] M.A. Amirabadi, V.T. Vakili, Performance analysis of a novel hybrid FSO/RF communication system, arXiv preprint arXiv:1802.07160v2, (2018).
[19] N. Varshney, P. Puri, Performance analysis of decode-and-forward-based mixed MIMO-RF/FSO cooperative systems with source mobility and imperfect CSI, J. Lightwave Technol. 35 (11) (2017) 2070–2077.
[20] K. Kumar, D.K. Borah, Quantize and encode relaying through FSO and hybrid FSO/RF links, IEEE Trans. Veh. Technol. 64 (6) (2015) 2361–2374.
[21] M.A. Amirabadi, V.T. Vakili, Performance of a Relay-Assisted Hybrid FSO/RF Communication System. arXiv preprint arXiv:1803.00711, (2018).
[22] J. Zhang, L. Dai, Y. Zhang, Z. Wang, Unified performance analysis of mixed radio frequency/free-space optical dual-hop transmission systems, J. Lightwave Technol. 33 (11) (2015) 2286–2293.
[23] Z. Jing, Z. Shang-hong, Z. Wei-hu, C. Ke-fan, Performance analysis for mixed FSO/RF Nakagami-m and exponentiated Weibull dual-hop airborne systems, Opt. Commun. 392 (2017) 294–299.
[24] G. Djordjevic, M. Petkovic, A. Cvetkovic, G. Karagiannidis, Mixed RF/FSO relaying with outdated channel state information, IEEE J. Sel. Areas Commun. (2015).
[25] L. Kong, W. Xu, L. Hanzo, H. Zhang, C. Zhao, Performance of a free-space-optical relay-assisted hybrid RF/FSO system in generalized m-distributed channels, IEEE Photonics J. 7 (5) (2015) 1–19.
[26] T.A. Tsiftsis, H.G. Sandalidis, G.K. Karagiannidis, N.C. Sagias, Multihop free-space optical communications over strong turbulence channels, in: Communications, 2006. ICC'06. IEEE International Conference on, 2006, pp. 2755–2759.
[27] P. Wang, T. Cao, L. Guo, R. Wang, Y. Yang, Performance analysis of multihop parallel free-space optical systems over exponentiated Weibull fading channels, IEEE Photonics J. 7 (1) (2015) 1–17.
[28] M.A. Kashani, M. Uysal, Outage performance of FSO multi-hop parallel relaying, in: Signal Processing and Communications Applications Conference (SIU) 2012 20th IEEE, 2012, pp. 1–4.
[29] M.A. Kashani, M. Uysal, Outage performance and diversity gain analysis of free-space optical multi-hop parallel relaying, J. Opt. Commun. Netw. 5 (8) (2013) 901–909.
[30] G. Farhadi, N.C. Beaulieu, Capacity of amplify-and-forward multi-hop relaying systems under adaptive transmission, IEEE Trans. Commun. 58 (3) (2010).
[31] B. Makki, T. Svensson, M. Brandt-Pearce, M.S. Alouini, Performance analysis of RF-FSO multi-hop networks, arXiv preprint arXiv:1703.07166, (2017).
[32] M. Najafi, V. Jamali, R. Schober, Optimal relay selection for the parallel hybrid RF/FSO relay channel: non-buffer-aided and buffer-aided designs, IEEE Trans. Commun. 65 (7) (2017) 2794–2810.
[33] H. Kazemi, M. Uysal, F. Touati, H. Haas, Outage performance of multi-hop hybrid FSO/RF communication systems, in: Optical Wireless Communications (IWOW), IEEE 4th International Workshop on, 2015, pp. 83–87.
[34] B. Makki, T. Svensson, M.B. Pearce, M.S. Alouini, On the performance of millimeter wave-based RF-FSO multi-hop and mesh networks, IEEE Trans. Wirel. Commun. 16 (12) (2017) 7746–7759.
[35] E. Zedini, H. Soury, M.S. Alouini, Dual-hop FSO transmission systems over gamma–gamma turbulence with pointing errors, IEEE Trans. Wirel. Commun. 16 (2) (2017) 784–796.
[36] E. Zedini, I.S. Ansari, M.S. Alouini, Performance analysis of mixed nakagami-m and Gamma–Gamma dual-hop FSO transmission systems, IEEE Photonics J. 7 (1) (2015) 1–20.
[37] Wolfram, The Wolfram functions site, Available: http://functions.wolfram.com.
[38] A. Papoulis, S.U. Pillai, Probability, Random Variables, and Stochastic Processes, Tata McGraw-Hill Education, 2002.
[39] M.R. Bhatnagar, Z. Ghassemlooy, Performance analysis of gamma–gamma fading FSO MIMO links with pointing errors, J. Lightwave Technol. 34 (9) (2016) 2158–2169.